

AD-A097 818

CHARLES STARK DRAPER LAB INC CAMBRIDGE MA
MATERIALS RESEARCH FOR ADVANCED INERTIAL INSTRUMENTATION. TASK --ETC(U)
DEC 80 D DAS, K KUMAR, E WETTSTEIN
R-1435

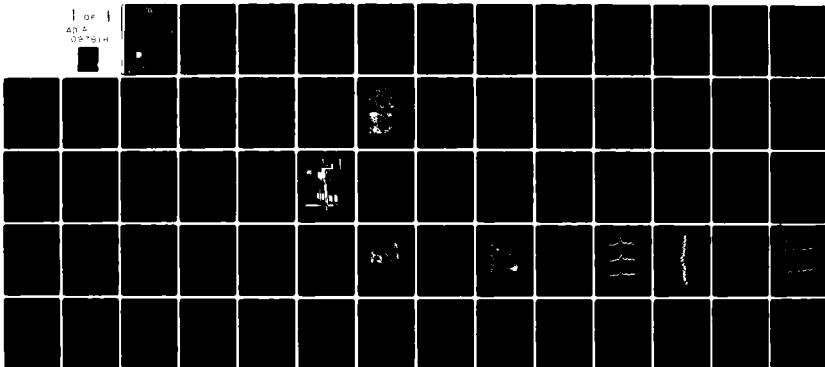
F/G 20/3

N00014-77-C-0388

NL

UNCLASSIFIED

1 of 1
43 4
08 214



END
DATE
FILMED
5-81
DTIC

LEVEL III

8656804
12

AD A 097 818

R-1435

**MATERIALS RESEARCH FOR ADVANCED
INERTIAL INSTRUMENTATION**

**TASK 3: RARE EARTH MAGNETIC MATERIAL
TECHNOLOGY AS RELATED TO
GYRO TORQUERS AND MOTORS**

DECEMBER 1980

TECHNICAL REPORT NO. 3
FOR THE PERIOD
1 OCTOBER 1979 - 30 SEPTEMBER 1980

BY

D. DAS, K. KUMAR, AND E. WETTSTEIN

DTIC
SELECTED
APR 16 1981
C

Prepared for the Office of Naval Research, Department of the Navy,
Under Contract N00014-77-C-0388

Approved for Public Release, Distribution Unlimited.

Permission is Granted the U.S. Government to Reproduce This
Paper in Whole Or in Part.



The Charles Stark Draper Laboratory, Inc.
Cambridge, Massachusetts 02139

81 4 16 007

DTIC FILE COPY

5

UNCLASSIFIED

SECURITY CLASSIFICATION OF THIS PAGE (When Data Entered)

⑨ Technical rept. no. 3, 2 Oct 79 - 30 Sep

80s

REPORT DOCUMENTATION PAGE		READ INSTRUCTIONS BEFORE COMPLETING FORM
1. REPORT NUMBER Technical Report No. 3 ✓	2. GOVT ACCESSION NO. AD-A094 878	3. RECIPIENT'S CATALOG NUMBER
4. TITLE (and Subtitle) Materials Research for Advanced Inertial Instrumentation, Task 3, Rare Earth Magnetic Material Technology as Related to Gyro Torquers and Motors	7. AUTHOR(s) D./Das, K./Kumar E./Wettstein	5. TYPE OF REPORT & PERIOD COVERED Research Report 10/1/79 - 9/30/80
		6. PERFORMING ORG. REPORT NUMBER R-1435
9. PERFORMING ORGANIZATION NAME AND ADDRESS The Charles Stark Draper Laboratory, Inc. ✓ 555 Technology Square Cambridge, Massachusetts 02139	11. CONTROLLING OFFICE NAME AND ADDRESS Office of Naval Research Department of the Navy 800 N. Quincy Street, Arlington, Virginia 20217	8. CONTRACT OR GRANT NUMBER(s) N00014-77-C-0388
		10. PROGRAM ELEMENT, PROJECT, TASK AREA & WORK UNIT NUMBERS 12) 691
14. MONITORING AGENCY NAME & ADDRESS (if different from Controlling Office) Office of Naval Research Boston Branch, Bldg. 114, Sec. D 666 Summer Street Boston, MA 02210	15. SECURITY CLASS. (of this report) Unclassified	12. REPORT DATE December 1980
		13. NUMBER OF PAGES 66
16. DISTRIBUTION STATEMENT (of this Report) Approved for public release, distribution unlimited		
17. DISTRIBUTION STATEMENT (of the abstract entered in Block 20, if different from Report)		
18. SUPPLEMENTARY NOTES		
19. KEY WORDS (Continue on reverse side if necessary and identify by block number)		
SmCo ₅ Magnets	Sintering	Flux Stability
Sm ₂ Co ₁₇ Magnets	Temperature Compensated Magnets	
Hot Isostatic Pressing	Thermal Expansion Coefficient	
Arc Plasma Spraying	Permanent Magnets	
20. ABSTRACT (Continue on reverse side if necessary and identify by block number) Hot isostatic pressing (HIP) of SmCo ₅ magnets can now be considered a viable alternative to sinter technology. Qualities of magnets are usually better. Even in as-HIPed condition the magnetic properties compare favorably with commercial sintered magnets. Thermal optimization following the HIP procedure further improves the properties. Unique in these magnets, as opposed to sintered magnets, are the consistently high H _c values obtained over the (Continued on reverse side)		

2025 316

A

slt

entire composition range of 35.5 to 37.0 weight percent Sm. It was interesting to note that the higher Sm compositions showed very little degradation of coercivity on slow cooling from aging temperature.

Flux decay rates were measured on a sinter magnet (which showed high H_{ci} and H_k) and a HIPed magnet (which was prepared from large particle size powder). Different thermal treatments were given to the magnet samples prior to magnetization and testing. The best results obtained corresponded to decay rates of 280 ppm/decade of days for the sinter magnets and 161 ppm/decade of days for the HIPed magnets. These low rates of decay were obtained when the samples were slow cooled following the aging treatment at 900° C.

Initial sinter experiments were performed to determine the compositions necessary to obtain zero temperature coefficient using $ErCo_5$ and $TbCo_5$ to replace part of $SmCo_5$. The zero compositions were determined; however the energy products corresponding to these compositions were low. Attempts are now being made to obtain higher values for the energy products by using the HIP technique.

Our highest energy product magnets prepared by HIP (21 MGOe) and sinter technique (18 MGOe) were measured for thermal expansion coefficient and found to have values within two percent of that of beryllium. There is, therefore, no need to sacrifice a part of the energy product to match the thermal expansion coefficients.

Investigation of the fabrication feasibility of Sm_2Co_{17} -type binary composition magnets with coercivities well in excess of those achievable by sintering procedures was included in this program in October 1979. Initial experiments showed that deposits which exhibit x-ray diffraction patterns characteristic of amorphous materials can be produced using this process in the composition range of interest. The possibility of producing magnets with the easy magnetization axis of the Sm_2Co_{17} phase oriented perpendicular to the plane of the deposit was indicated in some of the x-ray data. It was tentatively concluded that the cooling conditions at the substrate substantially affected the texture in the deposit. Low temperature treatments, which employed temperature as well as time at temperature variations, of the several deposited materials showed that coercivities substantially higher than the 1 to 2 kOe typically observed for the sintered " Sm_2Co_{17} -type" materials could be produced by this technique. The largest H_{ci} value measured in this program was for a deposit containing about 29.0 weight percent Sm (after making corrections for the estimated loss to evaporation and oxidation). This value was 7.9 kOe and was measured after exposing the deposited material to 600°C for 48 hours. The other magnetic properties of this deposit were $B_R = 6500$ G, $H_C = 4050$ Oe, and $(BH)_{max} = 6.6$ MGOe. Controlled crystallization studies on the amorphous deposits and deposition at temperatures other than those employed so far are planned.

R-1435

MATERIALS RESEARCH FOR ADVANCED INERTIAL INSTRUMENTATION

TASK 3: RARE EARTH MAGNETIC MATERIAL TECHNOLOGY
AS RELATED TO GYRO TORQUERS AND MOTORS

DECEMBER 1980

TECHNICAL REPORT NO. 3

FOR THE PERIOD

October 1, 1979 to September 30, 1980

by

D. Das, K. Kumar, and E. Wettstein

Prepared for the Office of Naval Research
Department of the Navy, under Contract N00014-77-C-0388

Approved for Public Release; distribution unlimited

Permission is granted to the U.S. Government to reproduce this report in
whole or in part.

Approved:


M.S. Sapuppo, Head
Component Development
Department

THE CHARLES STARK DRAPER LABORATORY
CAMBRIDGE, MASSACHUSETTS 02139

ACKNOWLEDGEMENTS

We wish to express our appreciation to the National Magnet Laboratory, MIT, for their assistance by making their high-field magnets available for our studies in this program. Our sincere thanks to C.R. Dauwalter for carrying out the flux stability measurements.

This report was prepared by The Charles Stark Draper Laboratory, Inc., under Contract N00014-77-C-0388 with the Office of Naval Research of the Department of the Navy, with Dr. F.S. Gardner of ONR, Boston, serving as Scientific Officer.

Publication of this report does not constitute approval by the U.S. Navy of the findings or conclusions contained herein. It is published for the exchange and stimulation of ideas.

Accession For	
NTIS GSA&I	<input checked="" type="checkbox"/>
DTIC TAB	<input type="checkbox"/>
Unannounced	<input type="checkbox"/>
Justification	
By _____	
Distribution/	
Availability Codes	
Dist	Avail and/or Special
A	

TABLE OF CONTENTS

<u>Section</u>	<u>Page</u>
1.	INTRODUCTION.....1
1.1	Program Background.....1
1.2	Objectives.....2
2.	PROGRESS PRIOR TO THIS REPORT.....5
3.	SmCo ₅ MAGNET INVESTIGATIONS DURING THIS REPORTING PERIOD.....9
3.1	Further Studies of Hot Isostatic Pressing (HIP) of SmCo ₅9
3.2	Results and Discussion of SmCo ₅ HIP Studies.....10
3.3	Flux Stability Measurements.....15
3.4	Discussion and Conclusions Regarding Flux Stability Measurements.....20
3.5	Temperature Compensated SmCo ₅ Magnets.....21
3.6	Thermal Expansion Control of SmCo ₅ Magnets.....31
3.7	Future Plans.....32
4.	Sm ₂ Co ₁₇ MAGNET INVESTIGATIONS.....35
4.1	General.....35
4.2	Background.....35
4.3	Rationale for Adopted Approach.....37
4.4	The Plasma Spray Process.....40
4.5	Results and Discussion.....41
4.6	Conclusions.....55
4.7	Recommendations for Future Work.....56
	REFERENCES.....57
	DISTRIBUTION LIST.....61

LIST OF FIGURES

<u>Figure</u>		<u>Page</u>
1	Optical micrograph of 40 μm particle size HIPed magnet after treatment at 1000°C for 75 hours.....	13
2	Optical micrograph of 25 μm particle size HIPed magnet after treatment at 1108°C for 3 hours.....	13
3	Magnetization as a function of temperature for SmCo_5 and several (HRE) Co_5 compounds.....	23
4	A schematic view of the apparatus for magnetic temperature coefficient.....	25
5	An overall view of the temperature coefficient measurement facility.....	26
6	Composition vs. magnetic temperature coefficient of Er-Sm-Co magnets.....	29
7	Composition vs. magnetic temperature coefficient of Tb-Sm-Co magnets.....	30
8	Schematic sketch of spray process.....	40
9	Etched microstructures of as-received alloys.....	42
10	Microstructures of as-deposited samples.....	44
11	As-Sprayed x-ray patterns obtained on two deposits made with 34 wt % Sm and one with 30 wt % Sm powders.....	46
12	X-ray pattern showing single, sharp crystalline peak superposed on an essentially amorphous pattern.....	47
13	X-ray patterns of 34.0 deposited sample.....	49
14	Effect of temperature of treatment on H_{ci}	52
15	Effect of time of exposure at 600°C on the value of H_{ci}	54

LIST OF TABLES

<u>Table</u>	<u>Page</u>
1	Magnetic properties at 40 μm -particle magnets HIPed at 900°C.....11
2	Magnetic properties of 25 μm -particle magnets HIPed at 950°C.....12
3	Magnetic properties of no. 24 and no. H-5.....16
4	Thermal treatments of sinter no. 24 and HIP H-5.....17
5	Flux decay rate of H-5 and sinter no. 24 magnets.....19
6	Compositions of sinter mixtures.....27
7	Measured and theoretical B_r of Er-Sm-Co and Tb-Sm-Co magnets.....27
8	Thermal expansion coefficients of some CSDL SmCo_5 magnets.....32
9	Effect of temperature of treatment.....51
10	Effect of time at temperature.....53

SECTION 1

INTRODUCTION

1.1 Program Background

The Charles Stark Draper Laboratory, Inc. (CSDL) is involved in research and development over a broad spectrum of technology associated with guidance, navigation, and control for vehicles of all types. One of the areas of importance to advancements in inertial navigation systems is the improvement of magnetic devices serving critical functions in these systems. Samarium-cobalt magnet devices are used within inertial systems as components of the inertial instruments or sensors - the gyro and accelerometer - and as gimbal torque motors. As an example of the former category, samarium-cobalt permanent magnets are employed in the torque generator, or angular motion forcer, of the movable and buoyant member of the instrument. The torque generator is of cylindrical geometry, and in many designs the magnets are located on the moving member which must remain buoyant in fluid. Here the lower volume of the magnet impacts favorably on the overall size and weight of the completed instrument.

Rare-earth cobalt magnets, because of their large maximum energy product, $(BH)_{\max}$, are ideally suited for many other applications requiring high magnetic strength. Because of the large $(BH)_{\max}$ a lesser volume of magnet is required to produce a given amount of magnetic flux in a device.

In addition to their high energy product, magnets utilized in precision inertial instruments must also possess excellent long-term flux stability, insensitivity to temperature change, and physical properties compatible with beryllium. Because of its favorable strength-to-weight ratio, beryllium is the structural material of choice in modern inertial instruments.

A comprehensive program to develop samarium-cobalt magnets by powder-metallurgy techniques for applications as components in new and future generations of inertial instruments was initiated at the Draper Laboratory in October 1977 under the sponsorship of the Office of Naval Research. The objectives of the program were to develop improved sintering procedures to fabricate inertial-grade SmCo_5 magnets with improvements in three areas mentioned above: long-term flux stability, reduced temperature coefficient, and tailoring of the thermal expansion coefficient to match that of beryllium.

During the first two years (October 1977 to September 1979) the efforts in the magnetic materials task of the ONR materials research program focused on sintered and hot isostatically pressed magnets of the SmCo_5 composition. A new subtask was added as of October 1979 which would concentrate on $\text{Sm}_2\text{Co}_{17}$ magnets fabricated by the arc-plasma-spray process. The motivation behind this subtask was the earlier achievement of outstanding successes with SmCo_5 magnets using this process at CSDL.

1.2 Objectives

The objectives of the present program are to investigate the arc-plasma spray process for fabricating $\text{Sm}_2\text{Co}_{17}$ -type magnets and to develop improved sintering procedures to produce inertial-grade SmCo_5 magnets with improvements in the following areas:

(1) Long-term flux stability at constant temperature (140°F)

Desired: 0.008 ppm/90-day
Present capability: Sintered: ~ 1 ppm/day
Plasma Sprayed: 0.05 ppm/day

(2) Thermal stability of residual induction

Desired: 0.1 ppm/°F
Present capability: 300 ppm/°F

(3) Tailoring of thermal expansion coefficient

Desired, same as beryllium: 6.6 μ in./in. °F
Isotropic: 4.7 μ in./in. °F

- (a) Along magnetization direction: 3.1 μ in./in. °F
- (b) Normal to magnetization direction: 7.1 μ in./in. °F

SECTION 2

PROGRESS PRIOR TO THIS REPORT

Two interim annual reports^{(1,2)*} have been submitted, which described the progress in this area for a period of two years from October 1977 to September 1979. The highlights of this past performance are summarized below.

The three objectives of the program were to incorporate into SmCo_5 magnets produced by powder metallurgy: (1) high flux stability, (2) near-zero temperature coefficient in the vicinity of the gyro-operating temperature, and (3) tailored thermal expansion coefficient to match that of beryllium. Of the three objectives, the achievement of high flux stability appeared to be the most challenging since there is a lack of adequate scientific understanding of the rather low values of flux stability typically measured in these magnets. Scientific basis for the other two objectives, in contrast, was quite clear^(3,4) and thus these objectives were considered more easily obtainable than the first one. Efforts during the first two years were therefore concentrated on the first objective, not only to achieve the stated goal but also to develop a scientific understanding of the phenomenon of flux decay in the SmCo_5 magnets.

Work began on the premise that to achieve high stability the magnets should also possess higher resistance to demagnetization, since the decay of magnetic induction is a demagnetization process. Hence, the values of coercivities, both H_{ci} and H_k , required improvement since these are a measure of the magnet's ability to resist demagnetization. Based on the understanding of the mechanisms of demagnetization in SmCo_5

*Superscripted numerals refer to sources in the List of References.

magnets, (5,6) the method of fabrication therefore needed to be improved. This entailed the development of a more sophisticated method of fabrication to maintain fine grain size while lowering the oxygen content in the finished magnet. The two requirements clearly conflicted each other. As a result, a compromise was sought which achieved an optimum combination of grain size and oxygen content.

In line with these requirements, a magnet sintering facility capable of ultra-high vacuum operation (10^{-6} torr capability at 1100°C) was designed and built for oxygen-free processing of these magnets. Techniques for producing powder with low oxygen contamination (from the environment) were also developed for this purpose. The total amount of oxygen incorporated into the powder was found to be less than what is obtained with conventional procedures.

This resulted in remarkably high values of H_{Ci} and H_k in sintered SmCo_5 magnets produced at Draper Laboratory. The unprecedented value of 29 kOe was measured for H_k in a few of these magnets as compared to 5 to 10 kOe found in most commercial magnets. The energy-product values of these magnets were, however, limited to about 13 MGOe because of poor alignment. Further investigations were expected to result in substantial improvements in the values of the energy product. By controlling the maximum level of oxygen content to about 0.6 weight percent, along with fine grain size in the final sintered product, we were able to produce some outstanding magnetic properties, such as $(\text{BH})_{\text{max}} \sim 20$ MGOe, $H_{Ci} \sim 50$ kOe, and H_k of 33.5 kOe. The result was a low flux decay rate of 700 ppm/decade of days. This translated into a decay rate of less than a ppm/day in the third decade of time, which is the decade of interest. With special stabilizing treatments planned, the stability value was expected to be improved further.

The arc-plasma-sprayed magnets with an oxygen content of about 0.15% possess a low decay rate of 50 ppm/decade. Unfortunately, their energy products are low because of the random grain orientation. Our immediate goal was to produce aligned and densified powder metallurgical

magnets with oxygen content typical of APS magnets. To accomplish that, CSDL developed a hot isostatic pressing process in this program, which resulted in nearly 100% dense magnets of fine and aligned grain structure with little if any oxygen pickup above that of the starting powder compact. Properties of magnets formed with very coarse powder (using this technique) were found to be quite comparable to what is available with sinter technology. With the use of finer-sized powder, magnets with outstanding properties and high flux stability were expected, provided a low level of oxygen could be maintained in the fine powders.

Experiments to determine the flux decay rate were started on some of the high coercivity sintered magnets. These studies were to be expanded to include samples of various magnetic characteristics with the hope of understanding the underlying mechanism of high flux stability. In the ensuing period, efforts were expected to be directed towards temperature compensation and tailoring of thermal expansion along with further studies on stability.

SECTION 3

SmCo₅ MAGNET INVESTIGATIONS DURING THIS REPORTING PERIOD

3.1 Further Studies of Hot Isostatic Pressing (HIP) of SmCo₅

Important metallurgical considerations for producing high coercivity are believed to be fine grain size and low oxygen content in the sintered body.⁽⁷⁾ Because of the high temperature (approximately 1120°C) at which the sintering is carried out to achieve the desired degree of densification, there is considerable grain growth in the sintered body. The particle size of powder used is usually between 5 and 10 μm, compared to 20 to 30 μm grain size in the sintered magnet. Finer powder cannot be used without further increasing the oxygen content of 0.5 to 1.0 weight percent found even in these rather coarse powders.

If the densification of the powder could be achieved at temperatures in the range of 900° to 950°C there would be no significant grain growth.⁽⁸⁾ This can be accomplished only if a compressive force is applied to the powder compact while it is at the densification temperature. Using sinter-grade powder, dense magnets could be produced (ending up with grain size ranging between 5 to 10 μm) with oxygen content similar to that of sintered magnets made from the same powder. Alternatively, use could be made of powder size as large as is found for the grains in the sintered magnets resulting in similar grain size as standard sintered magnets but with a much smaller oxygen content. In either case an improvement in the magnetic properties is expected.

For these experiments the selected average powder particle sizes were 40 and 25 μm , both produced by the conventional techniques of crushing, pulverizing, and attritor grinding. The 40 μm size powder particle was produced by a short period of final grinding, using the -400 mesh fraction of the powder which was roughly 50 percent of the total. The finer powder with an estimated average particle size of 25 μm was obtained using longer time attritor grinding. Nominal chemical compositions of the powders were adjusted to 35.5, 36.5, 37.5, and 38.5 weight percent Sm for the coarse powder and 35.5, 36.0, 36.5, and 37.0 weight percent Sm for the fine powder by blending the powders of 34.5 percent Sm and 42.0 percent Sm alloys. The blended powders were cold isostatically pressed into 0.5-inch diameter cylindrical rods after alignment in a 140 kOe field Bitter solenoid. The 40- μm size compacts were then transferred to thin-walled stainless steel containers which were evacuated, baked out, sealed, and hot isostatically pressed (HIPed) at 900°C in an argon pressure of 15,000 lb/in² for 2 hours. The removal by machining of the magnet samples from the stainless steel container resulted in cracking. This was solved by slicing the assembly into usable size and using EDM to produce specimens for measurement. The problem of cracking encountered with the stainless steel cans was subsequently eliminated by using cold rolled low carbon steel containers for the next batch of samples, which were HIPed at 950°C. To avoid contamination of the alloys during HIP procedure, the cold-pressed compacts were wrapped with thin tantalum foil. The HIPed samples were removed from the container by dissolving the container material in warm dilute HNO₃. The tantalum foil was then easily removed following this acid solution treatment. Magnetic properties were measured for both 40- and 25- μm samples in the as-HIPed condition as well as after various thermal treatments.

3.2. Results and Discussion of SmCo₅ HIP Studies

The magnetic properties of the 40- μm -particle size HIPed magnets are shown in Table 1. Similar data for the 25- μm particles are given in Table 2.

Table 1. Magnetic Properties of 40 μm -particle magnets HIPed at 900°C.

Thermal Treatment	Sm Content	35.5	36.5	37.5	38.5
	Properties	wt %	wt %	wt %	wt %
As HIP'ed	B_r (kG)	7.9	7.9	7.1	7.2
	H_{ci} (kOe)	4.0	5.0	5.0	5.0
	H_k (kOe)	1.5	4.0	4.0	4.0
	$(BH)_{max}$ MGOe	6	10	8	9
75 h at 1000°C + 900°C 4 h Quick Cooled	B_r (kG)	8.1	7.9	7.1	7.2
	H_{ci} (kOe)	27.0	25.0	8	5
	H_k (kOe)	12.0	7.0	5.0	8.0
	$(BH)_{max}$ MGOe	16	14	11	9
	% Theor. Density	99.1	99.2	99.8	100.0

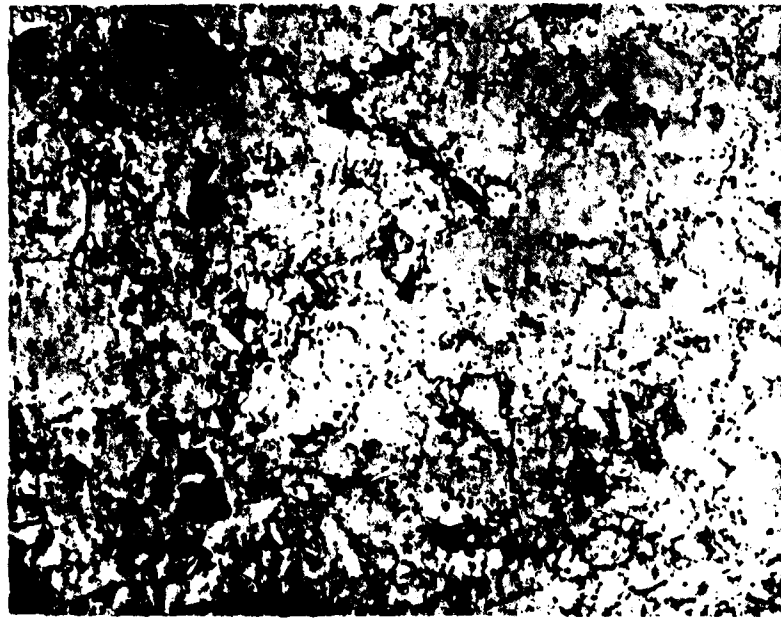
2/81 CD22600

In the as-HIPed condition the magnetic properties of 40- μm powder are poor and comparable to those of the raw powder. This indicated that the exposure to 900°C for 2 hours in HIP provided little or no healing of the damaged powder particles. However, it did produce a near-theoretical density with no grain growth. Figure 1 is an optical micrograph of the 35.5 percent Sm magnet of Table 1. The light grains are SmCo_5 and the darker ones are Sm_2Co_7 . The thermal treatment shown in Table 1 produced large increases in the coercivities of the 35.5 and 36.5 weight percent Sm magnets without changing the B_r , the grain size, or the grain morphology. These values are considered significant for magnets prepared out of such large particles of SmCo_5 powder. The high Sm-content alloys, however, did not show similar improvement in properties. Therefore, it was decided to investigate the range between 35.5 and 37.0 weight percent Sm with a somewhat smaller powder particle size (25 μm) HIPed at a slightly higher temperature (950°C). Near-theoretical density was reached, once again, with little grain growth.

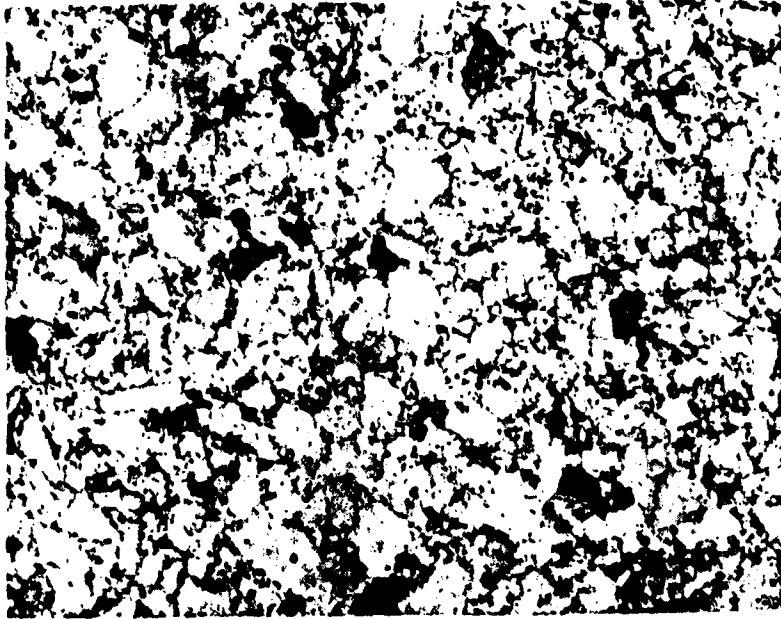
Table 2. Magnetic Properties of 25 μ m-particle magnets HIPed at 950°C.

Thermal Treatment	Sm Content Properties	35.5	36.0	36.5	37.0
		wt %	wt %	wt %	wt %
As- HIPed	B_r (kG)	8.9	8.6	8.6	8.4
	H_{ci} (kOe)	20	19	18	20
	H_k (kOe)	10	10	8	7
	$(BH)_{max}$ MGOe	20	19	17	16
950°C-62 h Quick Cooled	B_r (kG)	9.2	8.6	8.7	8.6
	H_{ci} (kOe)	36	36	34	35
	H_k (kOe)	19	14	12	10
	$(BH)_{max}$ MGOe	21	18	18	18
As Above Furnace Cooled	B_r (kG)	9.1	8.7	8.9	8.7
	H_{ci} (kOe)	18	26	29	31
	H_k (kOe)	6.5	8.0	7.5	8.5
	$(BH)_{max}$ MGOe	18	17	17	17
1050°C-24 h 900°C-24 h Quick Cooled	B_r (kG)	9	8.5	8.7	8.6
	H_{ci} (kOe)	33	35.5	33.5	33.5
	H_k (kOe)	26	20	17.5	18
	$(BH)_{max}$ MGOe	20	20	10	18
1108°C-3 h 900°C-24 h Quick Cooled	B_r (kG)	8.9	8.6	8.7	8.4
	H_{ci} (kOe)	33.5	36	33	32.5
	H_k (kOe)	25	24	18	17
	$(BH)_{max}$ MGOe	20	18	18	17
	% Theor. Density	98.7	99.1	98.7	99.3

2/81 CD22607



OPTICAL MICROGRAPH OF 40 μm PARTICLE
SIZE HIP'ed MAGNET AFTER TREATMENT
AT 1000 °C FOR 75 HOURS. NOMINAL COMPO-
SITION 35.5 wt % Sm.



OPTICAL MICROGRAPH OF 25 μm PARTICLE
SIZE HIP'ed MAGNET AFTER TREATMENT AT
1108 °C FOR 3 HOURS. NOMINAL COMPO-
SITION 35.5 wt % Sm.

2 81 CD22590

Figure 1.

Figure 2.

Various thermal treatments were given to a number of samples from each of the 25 μm HIPed ingots using a separate sample for each of the treatments. The magnetic properties of variously treated samples are summarized in Table 2, from which the following observations are made:

- (1) HIP at 950°C temperature induced a healing effect on the grains (similar to the sintering procedures at over 1100°C) with H_{ci} values in the range of 20 kOe.
- (2) Thermal treatments of 950°C for 62 hours, 1050°C for 24 hours, and 1108°C for 3 hours, each followed by 900°C aging and quick cooling produced higher values of coercivities.
- (3) Furnace cooling of the samples treated at 950°C degraded the coercivities significantly for lower Sm composition magnets (35.5 and 36.0 percent). The degradation was much less severe for the higher compositions (36.5 and 37.0 percent). The latter two samples are therefore expected to have a lower flux decay rate.
- (4) The B_r values show a decrease as the Sm-content is increased, as was expected because of the lowering of cobalt content. The slight changes in B_r values after different thermal treatments for a given composition, however, are believed to be due to slight inconsistencies in the alignment in the long cylindrical rods from which the various samples were cut, and not due to the thermal treatment itself.
- (5) The uniqueness of these magnets as opposed to those made by sintering⁽⁹⁾ are the nearly constant H_{ci} values over the entire range of composition of 35.5 to 37.0 weight percent Sm except, in one case, where the samples were furnace-cooled after a thermal treatment.

- (6) Microscopic examination of the HIPed magnets showed increasing amounts of Sm_2Co_7 phase with increasing Sm-content. The 35.5 percent Sm, 25 μm particle microstructure is shown in Figure 2. This is very similar to Figure 1, except for the smaller grain size. But in both the figures, the phase composition is consistent with the chemical composition.
- (7) The composition of all the HIPed samples was in the 2-phase field of Sm_2Co_7 and SmCo_5 . The presence of Sm_2Co_7 promotes densification during sintering at lower temperatures than would be necessary otherwise. The densification during HIP, on the other hand, is accomplished by means of compressive force, and therefore the role of Sm_2Co_7 in determining densification is expected to be minimal in this case.

3.3 Flux Stability Measurements

Measurement of flux decay rate had begun at the end of the last reporting period. Additional experimental measurements have been performed since then, and some significant improvements in the flux stability have been observed as a result of a few selected heat treatments of the magnets which were designed to lower the amount of dissolved oxygen in the SmCo_5 lattice. However, work is hampered by a lack of: (1) enough experimental facilities for flux decay rate measurement, and (2) facilities with the versatility needed for our purpose.

In order to obtain meaningful data, the experiment to measure the average decay rate of a given set of samples is usually carried on for as long as three months. With only one experimental apparatus available for such measurements, no more than about four measurements can be performed during a twelve month period. This is insufficient capability to determine the scientific basis for the flux decay mechanism in a short period of time. The large number of samples required for a single measurement in the present apparatus as also the way they are mounted in the magnetic circuit makes it difficult to give additional thermal

treatments, and it is nearly impossible to remagnetize the samples in situ. Both of the above operations would be possible in a new design conceived at CSDL some time ago.

Since measurements were limited to a very small number, it was necessary to be highly selective in choosing discrete samples with very specific thermal treatments in order to obtain significant information to determine the mechanism underlying the flux decay rates. The results obtained so far tend to indicate that the decay of flux in these magnets is a possible manifestation of the precipitation reaction of the dissolved oxygen in the SmCo_5 lattice. However, much more work needs to be done to ensure absolute confidence regarding this interpretation.

Flux decay rate measurements during this period have been made on a high coercivity die-pressed sintered magnet (no. 24) after several different thermal treatments prior to magnetization, and on one HIPed (no. H-5) magnet after a thermal optimization treatment followed by furnace cooling before magnetization. The thermally optimized intrinsic magnetic properties of the two magnets are shown in Table 3.

Table 3. Magnetic properties of no. 24 and no. H-5.

	no. 24	no. H-5
B_R (KG)	7.6	8.1
H_{ci} (kOe)	44.0	27.0
H_k (kOe)	33.5	12.0
$(BH)_{max}$ (MGOe)	14.4	16.0
wt % O_2	0.6	0.3

2/81 CD22602

Prior to machining of the material for producing flux decay rate measurement samples, the thermal treatments shown in Table 4 were given to the no. 24 sintered magnets and H-5 HIP magnets. These treatments produced the magnetic properties shown in Table 3.

Table 4. Thermal treatments of sinter no. 24 and HIP H-5.

Magnet	Thermal treatment
Sinter no. 24	1110°C-3 hr, 900°C-24 hr, quick cooled
H-5	1000°C-75 hr, 900°C-4 hr, quick cooled

2/81 CD22606

Two sets of flux stability samples of sinter number 24 and one set of H-5 were machined following the thermal treatments shown in Table 4. Of the two sets of number 24 samples, set number 2 (24-2) was given a stress-relieving thermal treatment of 480°C for 3 hours and this was followed by slow cooling. The set 24-1 was given a high temperature treatment of 1090°C for 2 hours followed by aging at 900°C for 24 hours and then was quick cooled. Quick cooling of samples was performed by pulling the samples out to a water cooled zone in the muffle, whereas slow cooling involved leaving the samples in the hot zone of the muffle after the furnace was turned off.

The samples were then magnetized in a 140 kOe field and were mounted on the outside wall of a Carpenter C-49 alloy cylinder. The mounting involved a bonding with an epoxy and curing at 150°C for 16 hours. The magnet cylinder was then introduced into a torque generator circuit and rotated at a constant speed over a period of time. The temperature of the measurement apparatus was carefully controlled at 140°F $\pm 0.1^\circ\text{F}$. The output voltage, which is proportional to the magnetic flux, was recorded. The decline of this voltage was then a direct measure of the decay of the magnetic flux. The change in the value of

this voltage expressed as parts per million of the initial value was plotted in a linear scale against log of time expressed in decades of days. With the proper empirical selection of zero time, the data could be represented by a straight line. The slope of the line gave the decay rate in ppm/decade of days.

After taking the initial data on sample 24-1 well into the second decade of time, the magnet assembly was taken out of the torque generator and given a 225°C treatment for 16 hours, and further decay rate data were taken on the set for approximately 110 days. The decay rate was observed to decrease about 10 percent of the previous value. Next, the magnet samples were removed from the C-49 mount and given the following heat treatment: 1108°C for 3 hours, lowered temperature to 900°C and held there for 24 hours. If the samples were quick cooled at this point, the magnets would be restored to the original structural condition with magnetic properties identical to those found during the first decay rate measurement experiment. Instead of quick cooling from the 900°C aging treatment, this time the samples were slow cooled. The slow cooling results in further precipitation of dissolved oxygen as Sm_2O_3 , and in formation of $\text{Sm}_2\text{Co}_{17}$, which causes some degradation of the coercivities, both H_{ci} and H_k .⁽²⁾ If, however, the decay of flux with time is dependent on phenomena such as oxygen precipitation and relief of residual stress, then such a treatment should produce a lower decay rate. The measurements of decay rate on 24-1 samples following the above thermal cycling did indeed significantly improve the flux stability.

After machining, the HIPed samples (H-5) were given a stress relief and structure restoration treatment at 1050°C followed by a 900°C aging and slow cooling. It is suspected that the slow cooling decreased the H_{ci} and H_k values shown in Table 1. The flux decay rate measurements of both the HIP H-5 and various thermally treated sinter magnets number 24 are presented in Table 5.

Table 5. Flux decay rate of H-5 and sinter no. 24 magnets.

Sample Number	Heat Treatment After Machining Before Magnetization	Heat Treatment After Magnetization and Mounting	Days From Last Heat Treatment To Start Of Measurement	Zero-time - Days Added To Start Of Measurement for Straight Line	Measurement Period - Days	Decay Rate $\frac{\rho_p}{\rho_0}$ / decade of days
24-2	480°C-3 hrs furnace cooled	Bonding + 150°C-16 hrs	15	15	35	813 ppm
24-1-1	1090°C-2 hrs, 900°C-24 hrs, quick cooled	Bonding + 150°C-16 hrs	29	6	27	761
24-1-2	Above mounted sample, 225°C-16 hrs following previous measurement		60	20	110	693
24-1-3	1108°C-3 hrs, 900°C-24 hrs, furnace cooled	Bonding + 150°C-16 hrs	25	25	35	280
H-5	1050°C-2 hrs, 90°C-24 hrs, furnace cooled	Bonding + 150°C-16 hrs	9	9	49	162

2/81 CD22603

3.4 Discussion and Conclusions Regarding Flux Stability Measurements

The linear relationship between the flux decay and time plotted on a log scale was suspected. When the data was plotted using the zero time as the time of start of the experiment, the resultant curve showed smaller slope at the beginning with increasing slope as time went on. It also appeared that if the experiment was run for a very long time (for example, about 4 decades of days), a log plot would eventually become a straight line with a constant slope. In order to obtain the desired result with measurements of shorter duration, one had to add some numbers of days to the starting time of measurement. That is what was done to obtain the straight line which showed the smallest deviation of the individual data points from a straight line. In Table 5, it is seen that three out of five sets of data could be reduced to the linear relationship if the starting time was assumed to be the time of the last heat treatment. Two sets of data, e.g., 24-1-1 and 24-1-2, show that the zero time started sometime after the last heat treatment.

It should also be noted that from the time the samples had seen their last heat treatment they were stored at room temperature ($\sim 23^{\circ}\text{C}$), which was considerably less than the measurement temperature of 60°C . Since the chemical reaction at 23°C is bound to be much slower, and therefore negligible, than at 60°C , the linear relationship should have been obtainable almost from the beginning of the measurement cycle at 60°C . The aging at 150°C for 16 hours to cure epoxy used for bonding may be responsible for making it appear that the start was actually earlier than the start of the measurement. To obtain more meaningful data, the sample should be stored at the temperature of measurement and should not be allowed to experience an appreciably higher temperature (as during the curing of the epoxy bonding) even for a short duration, which gives an aberration to the recorded data. It is, of course, not possible to do so with the present apparatus.

The difference in the decay rate between 24-1-1 and 24-1-2 indicates that thermal stabilization would have to be carried out at a substantially higher temperature than 225°C to achieve lower decay rate. The high decay rate seen in sample 24-2 is most probably due to higher residual stresses because of incomplete removal of machining effects by the 480°C thermal treatment.

The lowest values of decay rates were seen in H-5 and 24-1-3. Both of these sets were furnace cooled from the aging temperature of 900°C. Although this treatment decreases both H_{ci} and H_k , it does so by precipitating a portion of dissolved oxygen from the $SmCo_5$ lattice. The lower the dissolved oxygen, the lower would be the subsequent precipitation. Therefore, it appears that the lower the oxygen content in solid solution in $SmCo_5$, the lower would be its decay rate. Any thermal treatment which reduces dissolved oxygen (and residual stresses) is expected to provide more stable performance. The fact that the higher stabilities were achieved in these magnets as a result of thermal treatments, which in effect lowered the H_{ci} and H_k values, contradicts the conclusion by Mildrum and Wong⁽¹⁰⁾ that higher H_k values produce higher stability.

The total oxygen contents in sinter number 24 and HIP H-5 were 0.6 weight percent and 0.3 weight percent respectively. The belief at this time is that the oxygen content would have to be substantially reduced below these values in order to achieve a goal of even higher stability. In a program funded by NASA, we are now trying to develop a powder preparation and encapsulation technique which is expected to yield HIP'ed $SmCo_5$ magnets with extremely low oxygen content. Combining the efforts of both the ONR and NASA programs should allow us to reach the goals of very high stability for the ONR magnet program.

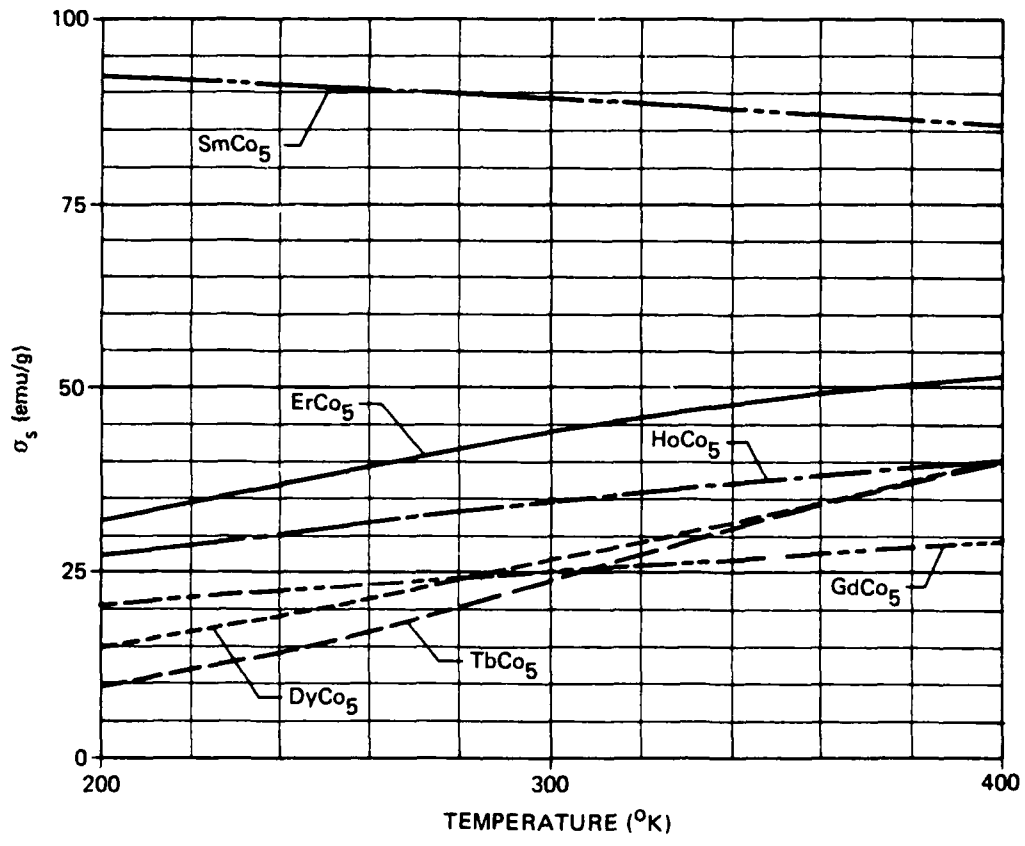
3.5 Temperature Compensated $SmCo_5$ Magnets

Loss of residual induction of a magnet, when taking it up to an elevated temperature below its Curie temperature, is composed of two

parts: irreversible and reversible. On cooling down to room temperature, the reversible loss is restored, but the irreversible loss can be regained only by remagnetization, provided there has been no structural change caused by the thermal cycling. Assuming that to be the case, the magnet, after the first thermal treatment, will retrace the same induction versus temperature curve on repeated thermal cycling between room temperature and the particular higher temperature.

SmCo_5 shows a continuous decrease of flux at a rate of approximately 400 ppm/°C within a temperature range of room temperature (RT) to 250°C. All heavy rare earth - cobalt alloys (HRE) Co_5 , such as ErCo_5 , HoCo_5 , DyCo_5 , GdCo_5 , and TbCo_5 , have an initial increase before they start to decrease towards zero at temperatures below the Curie temperature.^(11,12) From the above two references the data was replotted on saturation magnetization of the (HRE) Co_5 compounds along with those of SmCo_5 for the temperature range of 200°K to 400°K in Figure 3, which included the temperature of interest. Because of the opposite signs of temperature coefficients between that of SmCo_5 and the HRE Co_5 , one would expect that a rare-earth composition balanced between Sm and any of the HREs would result in a zero temperature coefficient.

Studies done elsewhere^(3,13) have shown such results using the two HRE elements Gd and Ho in conjunction with Sm. It takes approximately 20 percent Ho or 40 percent Gd to achieve a near-zero temperature coefficient. The slopes of TbCo_5 and ErCo_5 appear to be much higher than either HoCo_5 or GdCo_5 . It is therefore expected that a much smaller amount of ErCo_5 or TbCo_5 would achieve the zero temperature coefficient. The result, of course, will be that not as much of the energy product need be sacrificed. This is important in view of the fact that almost 50 percent of the energy product is lost when perfect temperature compensation is brought about by the addition of GdCo_5 . In the case of HoCo_5 the loss is still a third of the energy product. With ErCo_5 and TbCo_5 the loss of energy product is expected to be less than what has been found with HoCo_5 and GdCo_5 .



12/77 CD13030

Figure 3. Magnetization as a function of temperature for SmCo₅ and several (HRE)Co₅ compounds.

3.5.1 Experimental

The experiments carried out during the reporting period consisted of experimental determination of compositions in the two ternary systems Er-Sm-Co and Tb-Sm-Co for zero temperature coefficient, and devising a method for rapid measurement for screening the composition.

3.5.1.1 Measurement Apparatus

The principle used for the apparatus was the measurement of the change of flux in a gap, the flux being provided by the magnet being investigated. A double gap iron yoke was built, with a variable gap to accommodate the magnet and a fixed dimension gap where a high sensitivity Hall probe was located to measure the flux. A cutaway schematic drawing of the apparatus is shown in Figure 4. The gap with the magnet was located in a kerosene bath whose temperature could be varied over the range of 130°F to 170°F and controlled to within $\pm 0.1^\circ\text{F}$. The Hall probe gap was located in the upper chamber whose temperature was also controlled to a preselected constant value within $\pm 0.1^\circ\text{F}$, by means of water, ice, and a controlled speed stirrer. Thermocouples were located strategically to obtain precise measurement of the magnet and the Hall probe temperature. The instrumentation consisted of: (1) controlled variable speed motor for the stirrer, (2) temperature controlled kerosene bath, and (3) high precision digital read-outs of thermocouples and Hall probe output. The complete assembly is shown in Figure 5.

3.5.1.2 Determination of Temperature Compensated Magnet Composition

For gyro applications the temperature compensation is required for the small temperature range of 140°F to 160°F. From the magnetization versus temperature curves shown in Figure 3, rough estimates of the

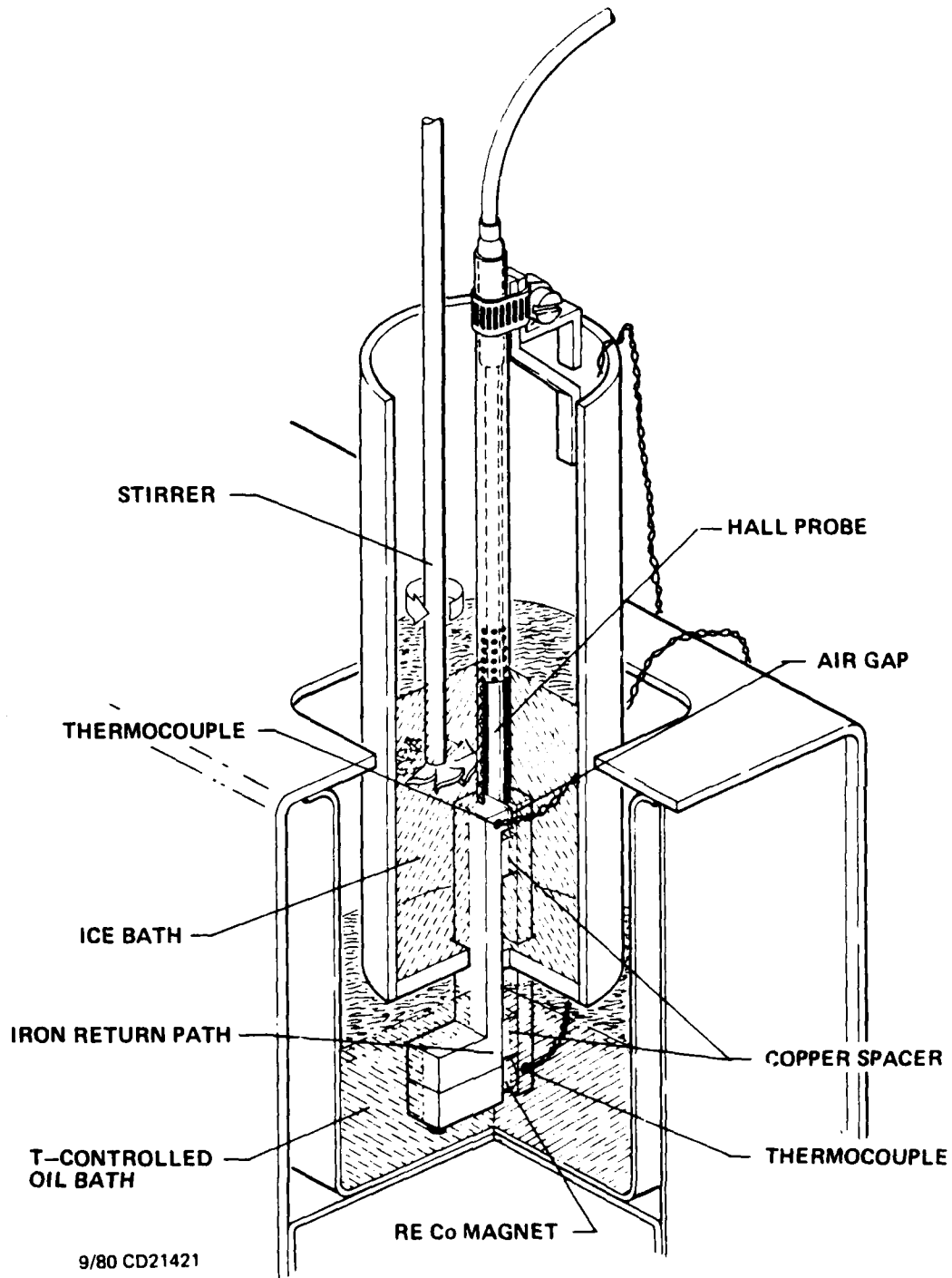
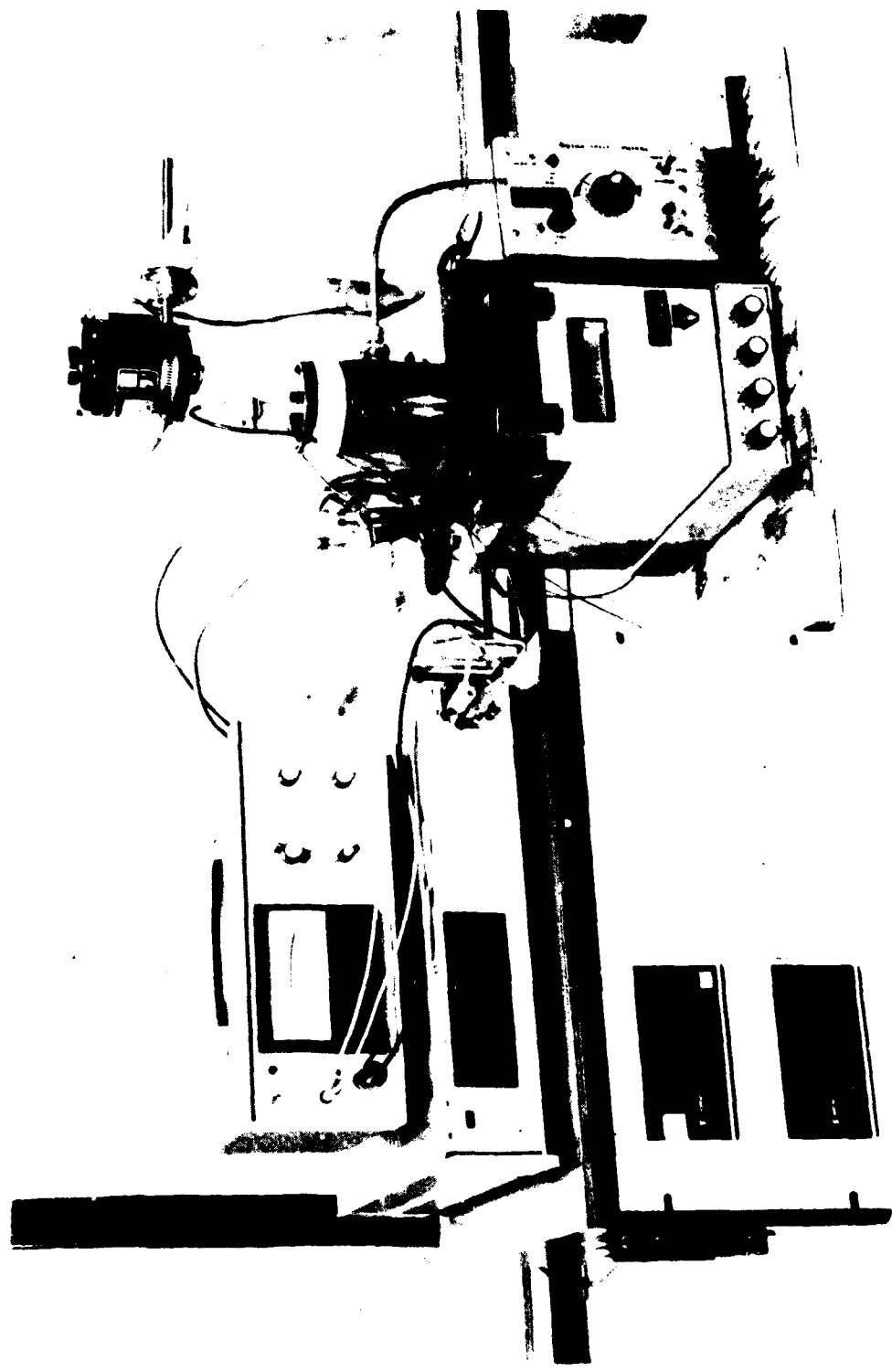


Figure 4. A cutaway schematic view of the apparatus for magnetic temperature coefficient.



CO21438

Figure 5. An overall view of the Temperature Coefficient Measurement Facility, showing temperature controllers and measurement instrumentation.

composition (expressed in weight percent of the respective compound) for zero coefficient were determined to be:

- (1) 33.3% ErCo₅ + 66.7% SmCo₅
- (2) 18.2% TbCo₅ + 81.2% SmCo₅

For the initial experiments, powder mixtures of ErCo₅ + SmCo₅ and TbCo₅ + SmCo₅ were prepared to give compositions on both sides of the compositions indicated above. Since the magnets were to be prepared by the sintering technique, the compositions were further adjusted with a 42.0 percent Sm alloy to maintain a 36.5 percent Sm equivalent of the rare earth elements, while still maintaining the ErCo₅/SmCo₅ and TbCo₅/SmCo₅ ratios as shown in Table 6.

Table 6. Compositions of sinter mixtures.

Mixture No.	ErCo ₅ wt %	Mixture No.	TbCo ₅ wt %
Er-1	23.3	Tb-1	8.2
Er-2	28.3	Tb-2	13.2
Er-3	33.3	Tb-3	18.2
Er-4	38.3	Tb-4	23.2
Er-5	43.3	Tb-5	28.2

2/81 CD22604

Table 7. Measured and theoretical B_r of Er-Sm-Co and Tb-Sm-Co magnets.

wt % Er of Total RE	Theor. B _r (G)	Measured B _r (G)	wt % Tb of Total RE	Theor. B _r (G)	Measured B _r (G)
23.3	8800	6950	8.2	9400	7500
28.3	8550	6400	13.2	9050	7100
33.3	8300	5600	18.2	8650	6750
38.3	8150	5450	23.2	8300	5300
40.0	8000	--	28.2	7950	5350
43.4	7800	5000	40.0	7100	--

2/81 CD22605

Several discs of each of the above compositions were prepared by die pressing in a 20 kOe aligning field. They were sintered at various temperatures. As indicated by the shrinkage of the die pressed discs, fairly good sintering for the Tb containing mixtures was obtained at sintering temperatures of 1130°C and higher. Er containing samples did not sinter well at even 1140°C, but were physically strong enough for both hysteresis loop as well as temperature coefficient measurements.

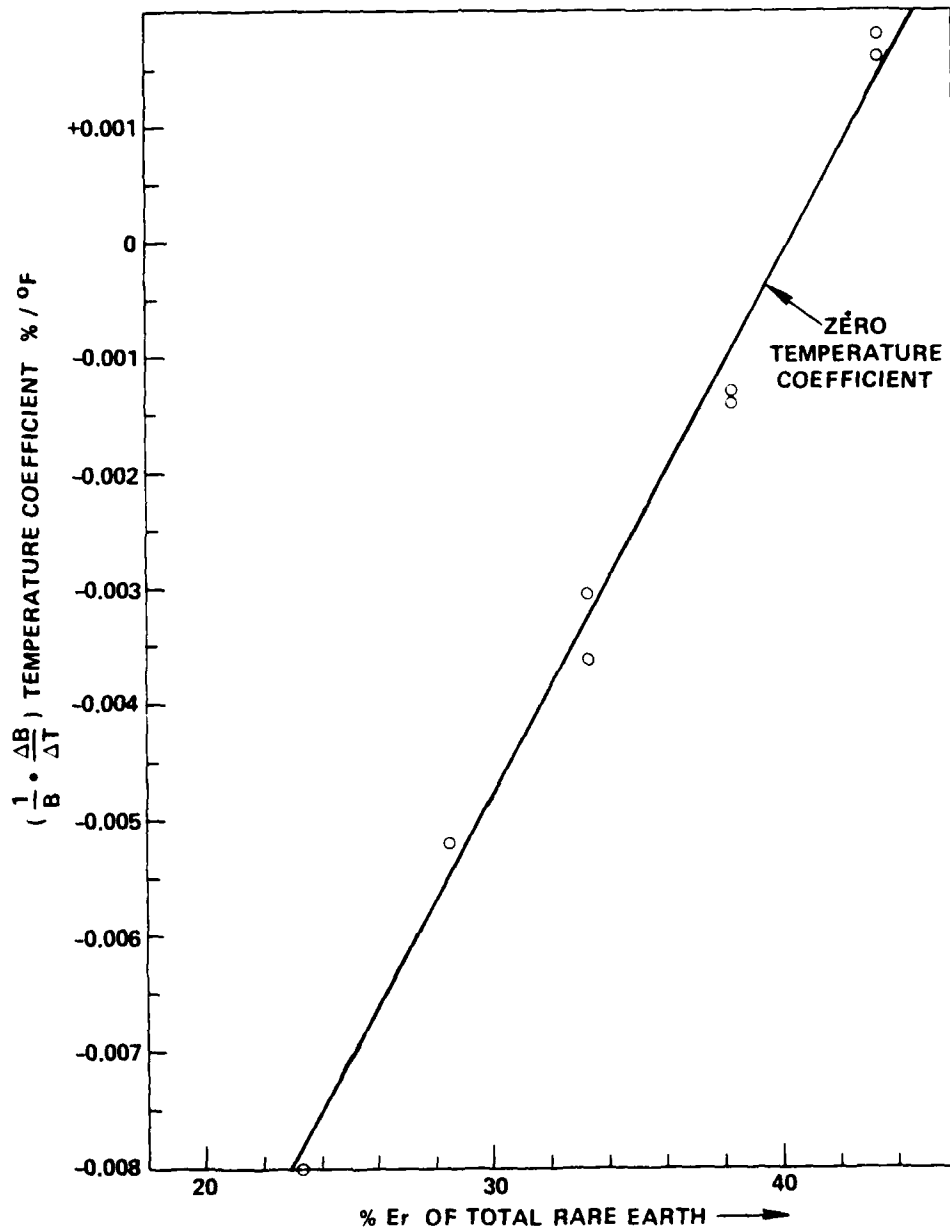
3.5.2 Results and Discussion

The two parameters of significance in these magnets are B_r and the temperature coefficient. The values of measured B_r are shown in Table 7 along with the theoretical values. In Figures 6 and 7 the temperature coefficients of Er and Tb respectively have been plotted against composition.

There are some discrepancies that were observed between measured and calculated values. The calculated values were based on reported properties in literature.

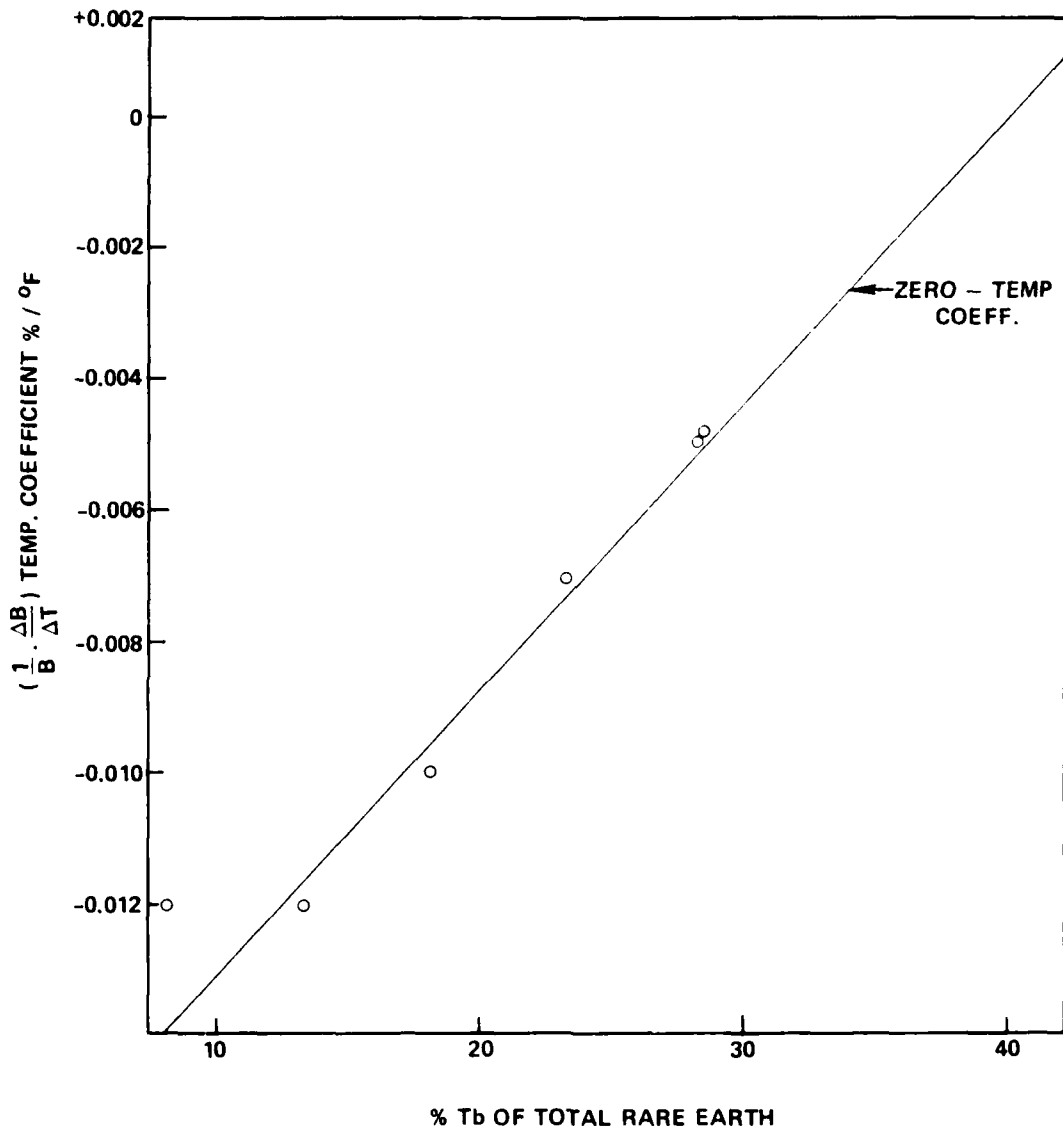
1. Zero temperature coefficients should have occurred at 33.3 percent Er and 18.2 percent Tb. From our results, the zero coefficient appears to be at 40 percent for either ternary system.
2. The measured values of B_r are substantially below the calculated values.

The die-pressed sintering technique used did not appear to produce satisfactory densification. Low B_r values could be explained on this basis and also due to poor alignment. HIP processing will undoubtedly remove some of the problem associated with the low B_r values. We do not, however, expect to solve the problem relating to composition by HIP processing. To explain this problem it will be necessary to determine the intrinsic properties of both $ErCo_5$ and $TbCo_5$ including their relationships between magnetization and temperature. We expect to concentrate on these areas in the ensuing period.



2/81 CD22577

Figure 6. Composition vs. magnetic temperature coefficient of Er-Sm-Co magnets. Zero temperature coefficient is shown by interpolation of data.



2/81 CD22579

Figure 7. Composition vs. magnetic temperature coefficient of Tb-Sm-Co magnets. Zero temperature coefficient is shown by extrapolation of data.

3.6 Thermal Expansion Control of SmCo₅ Magnets

One of the stated objectives of this program was to tailor the thermal expansion coefficient of the magnet to match that of beryllium. The purpose for this matching would be to reduce stresses at the bonded interface between the magnet and the beryllium support structure. For the magnet, the plane perpendicular to the magnetization direction is expected to be bonded to a beryllium surface, which would be the basal plane of the SmCo₅ hexagonal crystal. The thermal expansion coefficient of beryllium is $6.6 \times 10^{-6}/^{\circ}\text{F}$. The coefficient values for SmCo₅(4) magnets are as follows:

Parallel to C-axis	$3.1 \times 10^{-6}/^{\circ}\text{F}$
Perpendicular to C-axis	$7.1 \times 10^{-6}/^{\circ}\text{F}$
Isotropic	$4.7 \times 10^{-6}/^{\circ}\text{F}$

Since both the sintered and HIPed magnets are produced from aligned and cold compacted SmCo₅ powder, the plane perpendicular to the magnetization direction should have a thermal expansion coefficient α much greater than 4.7×10^{-6} and somewhat less than 7.1×10^{-6} .

It was decided to determine the thermal expansion coefficients of some of the SmCo₅ magnets that had been produced in the laboratory, as well as that of HIP 50 type beryllium. The results are shown in Table 8.

The thermal expansion values shown in Table 8 indicate that the best match with beryllium is obtained from the HIPed magnet and sinter sample number 20. It is felt that we have an adequate match of thermal expansion to avoid mechanical stress problems. It is also reassuring that energy product of the magnet will not have to be sacrificed in achieving the goal of thermal expansion match.

Table 8. Thermal expansion coefficients of some CSDL SmCo₅ magnets

Sample Number	Type*	B _r (KG)	(BH) _{max} MGOe	Thermal Expansion Coefficient in Basal Plane
H-26	HIP	9.2	21.0	6.7 x 10 ⁻⁶ /°F
24	D.P. Sintered	7.6	14.5	6.3 x 10 ⁻⁶ /°F
16	D.P. Sintered	7.8	15.0	6.2 x 10 ⁻⁶ /°F
20	D.P. Sintered	8.4	17.5	6.5 x 10 ⁻⁶ /°F
--	HIP Be	---	---	6.6 x 10 ⁻⁶ /°F

2/81 CD22608

- *HIP - hot isostatically pressed.
 D.P. Sintered - die pressed and sintered.
 CIP sintered - cold isostatically pressed and sintered.

However, we are now in the process of generating temperature compensated magnets by replacing a portion of SmCo₅ with either ErCo₅ or TbCo₅. Once high energy product magnets are obtained from these two ternary systems, the thermal expansion matching problem will require examination once again.

3.7 Future Plans

- (1) Continue studies on flux decay mechanisms.
- (2) Further improvement of flux stability
 - (a) Lowered oxygen content using facilities being built at CSDL under a NASA contract
 - (b) Further refinement of thermal treatments

- (3) Continue studies with HIPed temperature compensated magnets
 - (a) Determine necessary alloy composition
 - (b) Determine magnetic properties
 - (c) Establish optimum thermal treatment
 - (d) Measure decay rate and thermal expansion coefficient
- (4) Process standardization
- (5) Try ONR SmCo_5 magnets in CSDL instruments

SECTION 4

Sm₂Co₁₇ MAGNET INVESTIGATIONS

4.1 General

This task was included in the program in November 1979. Its objective is to investigate the feasibility of employing arc-plasma-spraying as a process for producing Sm₂Co₁₇ type magnets of binary Sm-Co compositions with coercivities considerably higher than the 1 to 2 kOe that are obtained through the conventional sintering process. Examination of plasma spraying for Sm₂Co₁₇ magnet fabrication was mainly motivated by our earlier successes with the SmCo₅ composition.

4.2 Background

Low values of the intrinsic coercivity, H_{ci} , and H_k (= value of the reverse field that corresponds to 90 percent of the remanent magnetization in the second quadrant) are known to be generally related to poor long-term and short-term magnet flux stability.^(10,14) Large H_{ci} values reflect a strong resistance to demagnetizing forces and large H_k values indicate square loop demagnetization behavior.

Sintering is the most widely used technology for producing SmCo₅ and Sm₂Co₁₇ type magnets. The sequence of operation includes generation of fine alloy powder, alignment and compaction of this powder in an applied magnetic field, and sintering of the compact to achieve high density. This technique is presently capable of producing SmCo₅ magnets with $(BH)_{max}$ of 16 to 20 mGOe⁽¹⁵⁾ and Sm₂(TM)₁₇ magnets with energy products of about 30 mGOe.⁽¹⁶⁾ (TM = Transition Metal.) In each of these instances, however, the value of H_{ci} measured is considerably lower than what appears to be theoretically possible with these materials. The maximum H_{ci} attainable is indicated by the value of the measured anisotropy field, H_A , in these materials. These values are about 350 kOe for SmCo₅ and close to 100 kOe for Sm₂Co₁₇.⁽¹⁷⁾ The

actual values obtained in these materials for sintered magnets are in the range of 15 to 35 kOe for SmCo_5 , 1 to 2 kOe for $\text{Sm}_2\text{Co}_{17}$, and only about 5 to 6 kOe for modified $\text{Sm}_2\text{Co}_{17}$ compositions. These low H_{ci} values have been attributed by various researchers to effects arising from oxidation, microcracking and grain growth.⁽⁷⁾ While these low H_{ci} values may be suited for some general applications, they are particularly discouraging for applications that demand constant flux over extended periods of time.

The origins of oxidation, microcracking, and grain growth can be traced to the processing that is employed in the fabrication of this material. For effective alignment, compaction, and sintering, the starting powder material needs to be of extremely fine size (less than 10 microns). Because of the large overall surface area introduced by reduction of the powder to these fine sizes, a substantial amount of oxygen pick-up is observed. Even after taking extreme precautions, oxygen levels in excess of 0.35 to 0.5 weight percent are found in the powder and therefore in the resulting magnets.⁽¹⁸⁾ Typical commercial magnets, however, have up to 2 weight percent oxygen. To avoid the harmful effects of oxygen (because of a resulting depletion of the rare earth) excess Sm is added to the overall composition. While this adjusts the gross composition, it also results in the formation of cobalt-depleted regions through an oxygen dissolution and reprecipitation process.⁽⁶⁾ These are low coercivity regions that permit easy magnetization reversal in the material resulting in a lower measured H_{ci} value.^(6,19)

Effects related to microcracking are more subtle and less understood. Since microcracking results in the formation of extra surface (and, therefore, more defects), it appears that microcracks will be sources of reverse domain nucleation and growth. These microcracks are believed to result from the same processes that result in crack formation during processing of brittle ceramics.⁽⁸⁾ Both macro- and micro-stresses (related to high quenching rates and thermal expansion anisotropy respectively) are believed to lead to stress concentrations that result in crack formation. Slow cooling is, therefore, the

preferred mode of treatment following high temperature exposure.(19,20) Micro-stresses relating to anisotropic thermal expansion of SmCo_5 are believed to be responsible for striation formation in this material at intermediate temperatures.(20) Microcrack formation is an indication of the level of stresses (macro- and micro-) present in the material. These stresses may be an additional source of low coercivity.

The strong dependence of H_{ci} on grain size is believed to be related to the increased amount of defects present in the average grain of the large grain sized material.(5) Since the smaller the grain size the smaller the probability for occurrence of a defect, small grain size material is expected to (and appears to indeed have) higher coercivity. Some grain growth is unavoidable in commercial magnets (which are produced by sintering) during shrinkage and densification of the compact. Even when great care is taken during sintering, the final grain size is about 20 to 30 microns as opposed to a pre-sintered average particle size of less than 10 microns. Experiments have also shown that the sintered material is very inhomogeneous chemically because of which large scale second phase precipitation occurs at intermediate temperatures resulting in considerably reduced values of H_{ci} .(20)

All of the effects discussed above are known to play a strong role in determining H_{ci} in SmCo_5 magnets. While the analysis is equally valid for magnets produced with $\text{Sm}_2\text{Co}_{17}$ type compositions, these aspects take on added significance in the fabrication of this latter material. Experimental efforts to produce reasonably high H_{ci} $\text{Sm}_2\text{Co}_{17}$ magnets have so far been very disappointing.

4.3 Rationale for Adopted Approach

The single most important parameter for successful inertial applications is magnet flux stability at gyro operating temperatures. Initial experiments at CSDL have shown that sprayed SmCo_5 magnets show a remarkably lower rate of flux decay than do commercial magnets.(21)

This is primarily the result of the very high quality of material that has been produced in this program. Sprayed SmCo_5 magnets, however, are isotropic and, therefore, the energy product of these magnets is close to half of what is obtained in the aligned, commercially fabricated material. To obtain a higher amount of flux from these magnets, one needs to either introduce texture in the deposits or to shift the material composition towards higher cobalt content (by spraying $\text{Sm}_2\text{Co}_{17}$ type of deposits).

An isotropic $\text{Sm}_2\text{Co}_{17}$ magnet is expected to show an energy product of about 10 to 12 MGOe as opposed to 7 to 9 MGOe measured in isotropic SmCo_5 material and 16 to 18 MGOe found for aligned commercial SmCo_5 magnets. An aligned $\text{Sm}_2\text{Co}_{17}$ magnet would obviously show much higher values.

To date, efforts employing sintering of aligned magnets have been unsuccessful in fabricating magnets with acceptable levels to the intrinsic coercivity (H_{ci}). The maximum value of H_{ci} measured on binary $\text{Sm}_2\text{Co}_{17}$ sintered material is about 1 to 2 kOe as opposed to a theoretical maximum possibility of about 100 kOe.⁽¹⁷⁾ In contrast, CSDL's sprayed SmCo_5 magnets have exhibited coercivities of 68 kOe.⁽⁷⁾ This research deals with the production of higher values of intrinsic coercivity using the plasma spray process for isotropic $\text{Sm}_2\text{Co}_{17}$ deposits with potential energy products on the order of 12 MGOe.

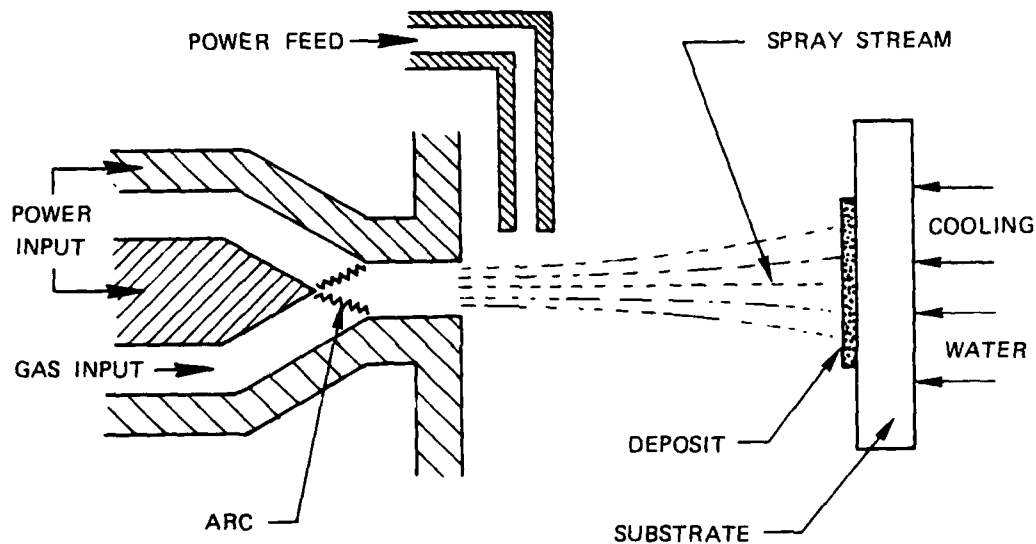
SmCo_5 magnets produced by spraying have demonstrated that these magnets can also be cooled slowly from high temperatures unlike sintered magnets that have to be cooled rapidly after treatment to avoid severe degradation in H_{ci} and in second quadrant demagnetization behavior.⁽¹⁹⁾ This degradation has recently been shown to result from increased second phase precipitation with decreasing temperatures because of existing chemical inhomogeneities.⁽²⁰⁾ Slow cooling leads to a decreased amount of strain in the material and therefore a lower incidence of crack formation.^(8,20)

The oxygen content of sprayed material is typically less than 0.2 weight percent mainly because spraying is conducted in an inert environment chamber and the starting powder (20 to 60 microns) is much larger than that used for sintering (less than 10 microns). An added advantage of this process is that while the starting size of the powder particle is large, the average grain size in the deposit is very small. Both amorphous and crystalline SmCo_5 material have been produced using this technique.^(22,23) Because of the fine grain size that is obtained, homogenization of the deposit occurs quite readily and very large values of H_{ci} are obtained by heating the deposited material to temperatures of 850°C to 1000°C, which are substantially lower than those required for sintering this material.^(1,15) This permits the retention of very fine grain sizes in sprayed magnets on the order of about 2 to 5 microns (compared to 20 to 30 microns in sintered material).⁽⁸⁾ All of these factors are believed to be responsible for the high H_{ci} values that have been obtained in sprayed SmCo_5 material.

The foregoing suggests that it might be possible to obtain reasonably large H_{ci} values in magnets sprayed with $\text{Sm}_2\text{Co}_{17}$ type compositions. H_{ci} values obtained in sprayed SmCo_5 material are about 20 percent of the anisotropy field. If a similar achievement can be attained in sprayed $\text{Sm}_2\text{Co}_{17}$ material, coercivities of about 15 to 20 kOe could result from such an effort (which would be larger than those obtained so far in sintered material by a factor of about 7 to 10). Such an improvement is desirable because it can result in sprayed magnets with energy products of about 10 to 12 mGOe and magnets of this type are expected to find many applications. Also, if additional subsequent efforts aimed at developing texture in these materials should prove successful, magnets with the highest magnetic properties attained so far will result.

4.4 The Plasma Spray Process

A schematic sketch of this process is shown in Figure 8. The process involves striking a high intensity dc arc between two electrodes, and ionization of gases - nitrogen, hydrogen, argon, and helium - as a consequence. This forms the plasma. Upon exit through a nozzle, the plasma combines to form neutral atoms, and releases a large amount of thermal energy without an appreciable loss in gas temperature. The material to be deposited is introduced at this stage in the form of a powder. The gases impart both thermal and kinetic energy to the powder particles, thereby melting them and propelling them rapidly towards the substrate to form the deposit.



10/77 12404 REV A 1/78

Figure 8. Schematic sketch of spray process. (22)

4.5 Results and Discussion

4.5.1 Alloy Procurement

The desired compositions of the deposits (after spraying) determined the compositions selected for the starting materials. Past experience with spray fabrication of these materials has shown that roughly 3 to 5 percent samarium is lost, relative to the cobalt (depending on the starting composition), through evaporation, during spraying. Also, an additional 1 percent is sacrificed to oxygen, both as a result of some oxygen present in the starting alloy and some that is picked up during processing. (The assumption that all of the oxygen in the deposit exists as an oxide of samarium appears reasonable in that Sm_2O_3 has the lowest free energy of formation amongst the several possible oxides that can be considered).

Based on these considerations, alloys with compositions containing 34.5, 25.2, and 23.5 weight percent Sm were ordered and procured from Research Chemicals, Phoenix, Arizona. It was recognized that the desired final deposit compositions should be in the range set by the stoichiometries of SmCo_5 (33.8% Sm) and $\text{Sm}_2\text{Co}_{17}$ (23.0% Sm) with the overall composition shifted towards the $\text{Sm}_2\text{Co}_{17}$ value. The as-received alloys were examined by optical microscopy. Figure 9 shows the etched microstructures of these alloy materials. Very large grains were observed. In two of the samples the existence of a second phase was observed. In the 25.2 weight percent Sm sample, the second phase appeared to exist mainly at the grain boundaries.

4.5.2 Deposit Fabrication

The alloys were crushed from ingot form to finer sizes using a laboratory jaw crusher and a double disk pulverizer. The resulting powder was sifted to select the correct size for spraying purposes. The several powders were mixed in a laboratory blender to secure as-blended

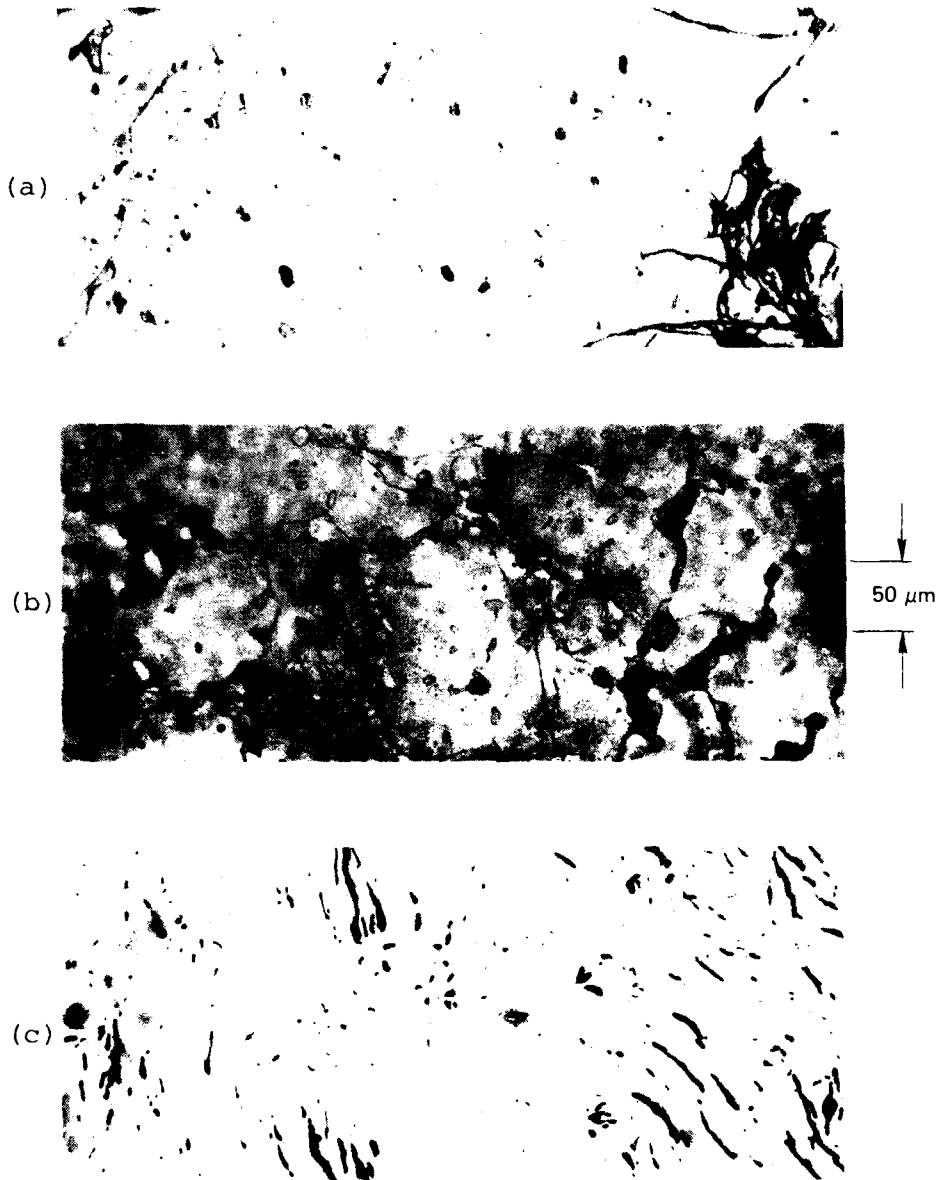


Figure 9. Etched microstructures of as-received alloys. (3) NiTi. (a) 34.5; (b) 35.5; (c) 36.5. (a) and (b) show existence of α phase. In (b) this is distributed at grain boundaries.

compositions of 34.0, 32.0, 30.0, 28.0, and 26.0 weight-percent samarium. Spray depositions were performed with these five starting powders on a copper substrate mounted on a water-cooled rotating feedthrough inside a water-jacketed, inert gas environment, plasma spray chamber. The conditions used for spraying were identical to those used previously for the SmCo_5 materials. These optimized conditions have evolved gradually over the past several years with our continued involvement in the spraying of the Sm-Co materials. The thickness of the as-sprayed deposits was typically about 0.3 cm. The samples were kept reasonably thin on purpose, since a greater level of crystallinity is known to develop in plasma-sprayed deposits with increasing deposit thickness during spraying.⁽²²⁾ The deposited material was removed from the copper substrate and characterized using a variety of techniques.

4.5.3 Microstructure

Sample pieces were removed from each of the deposits and metallographic specimens obtained to reveal the deposit cross-section. (Viewing axis was perpendicular to the plasma spray beam axis.)

Figure 10 shows the etched surfaces of the several deposit cross-sections. The nomenclature used in this report for deposit identification is 26.0 for deposits made from a starting powder of 26.0 weight-percent samarium composition, 30.0 for deposits produced from 30.0 weight-percent samarium powder, and so forth. The microstructures appear with a pancake-type morphology resulting from flattening of the molten alloy particles upon impact at the substrate.^(7,22) The as-sprayed structures also contain pores (which appear as dark, almost circular, regions) and a few unmelted particles, in addition to the observed platelets which give rise to the layered microstructure. The minor differences observed for the several deposit microstructures were not considered to be very significant.

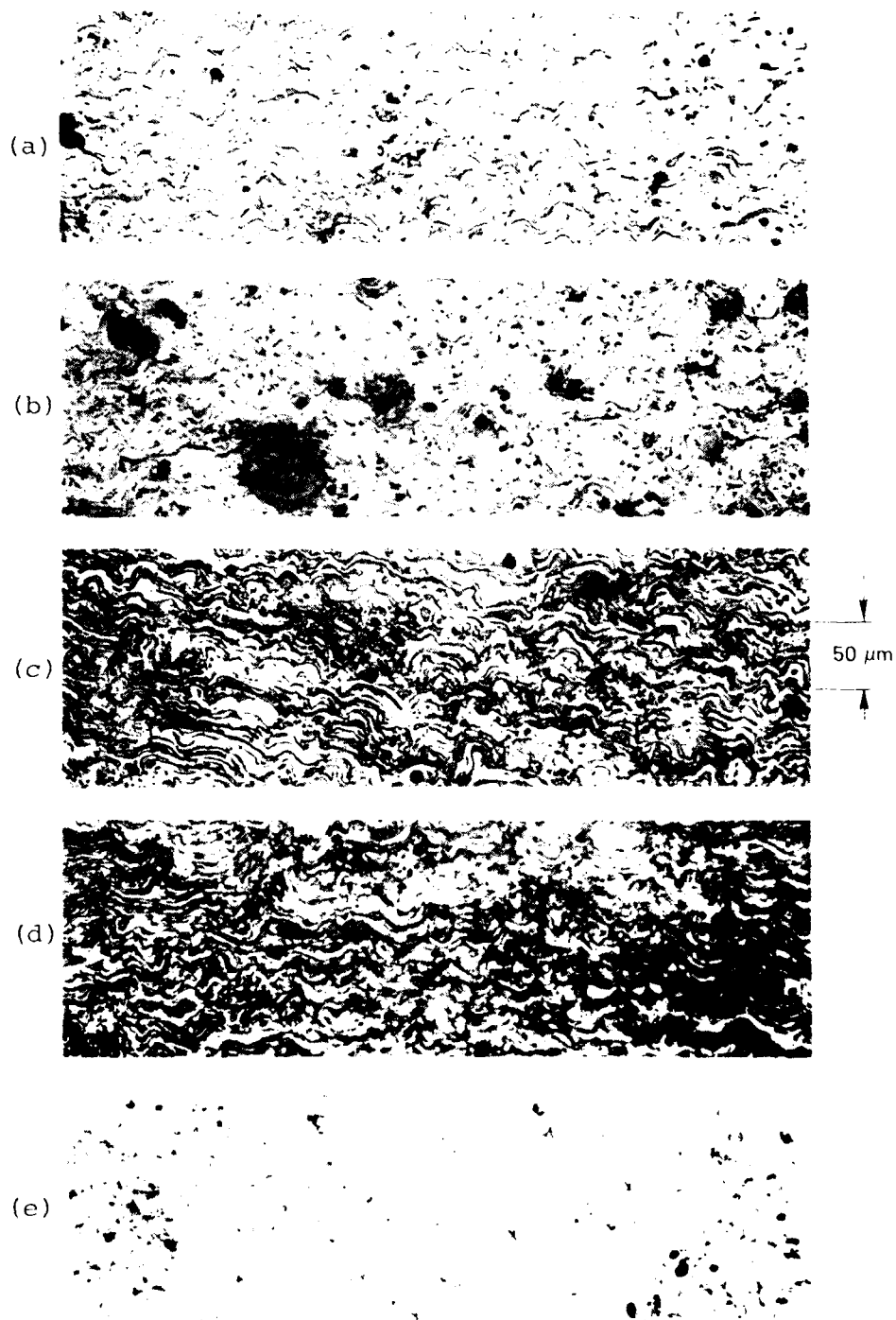
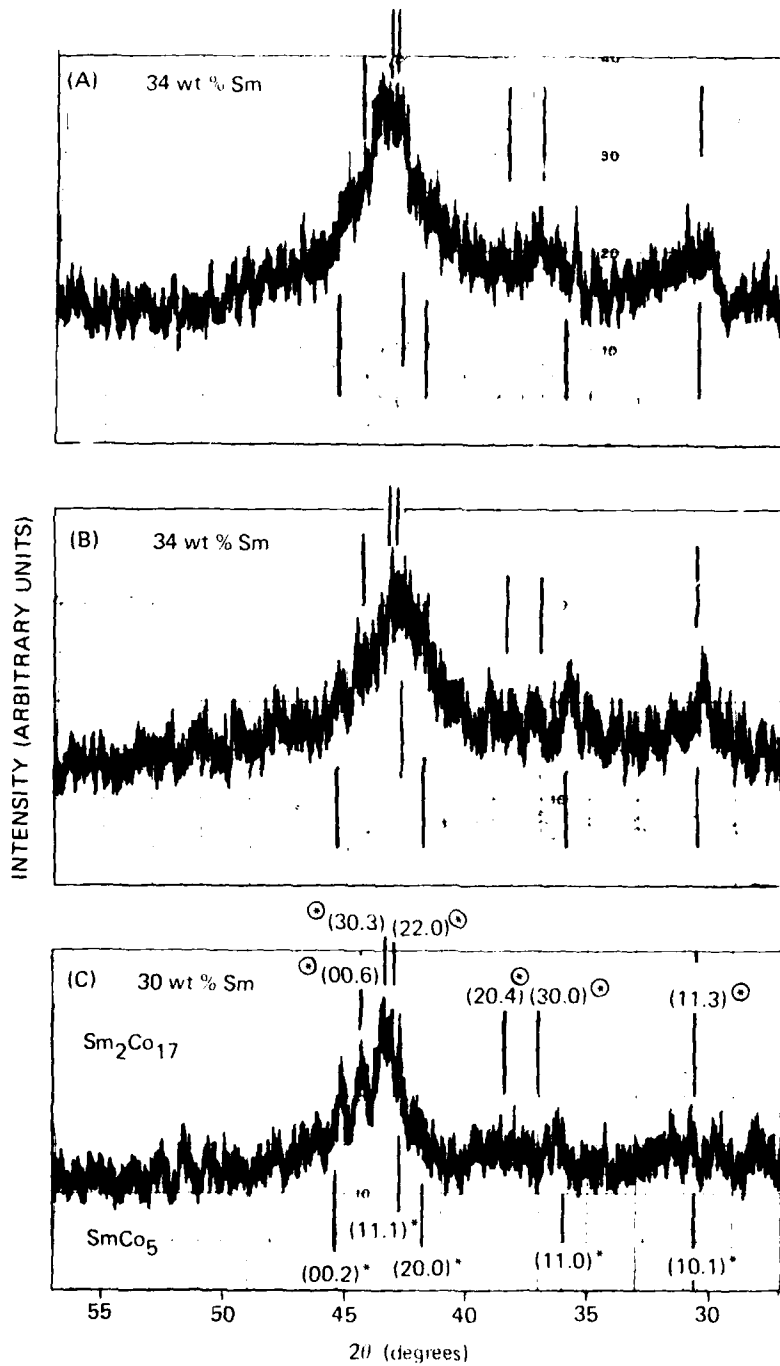


Figure 10. Microstructure of an S-100-140-1-amp 10.0% Nitral.
 (a) 34.0; (b) 34.0; (c) 34.0; (d) 34.0; (e) 34.0.

4.5.4 Crystal Structures

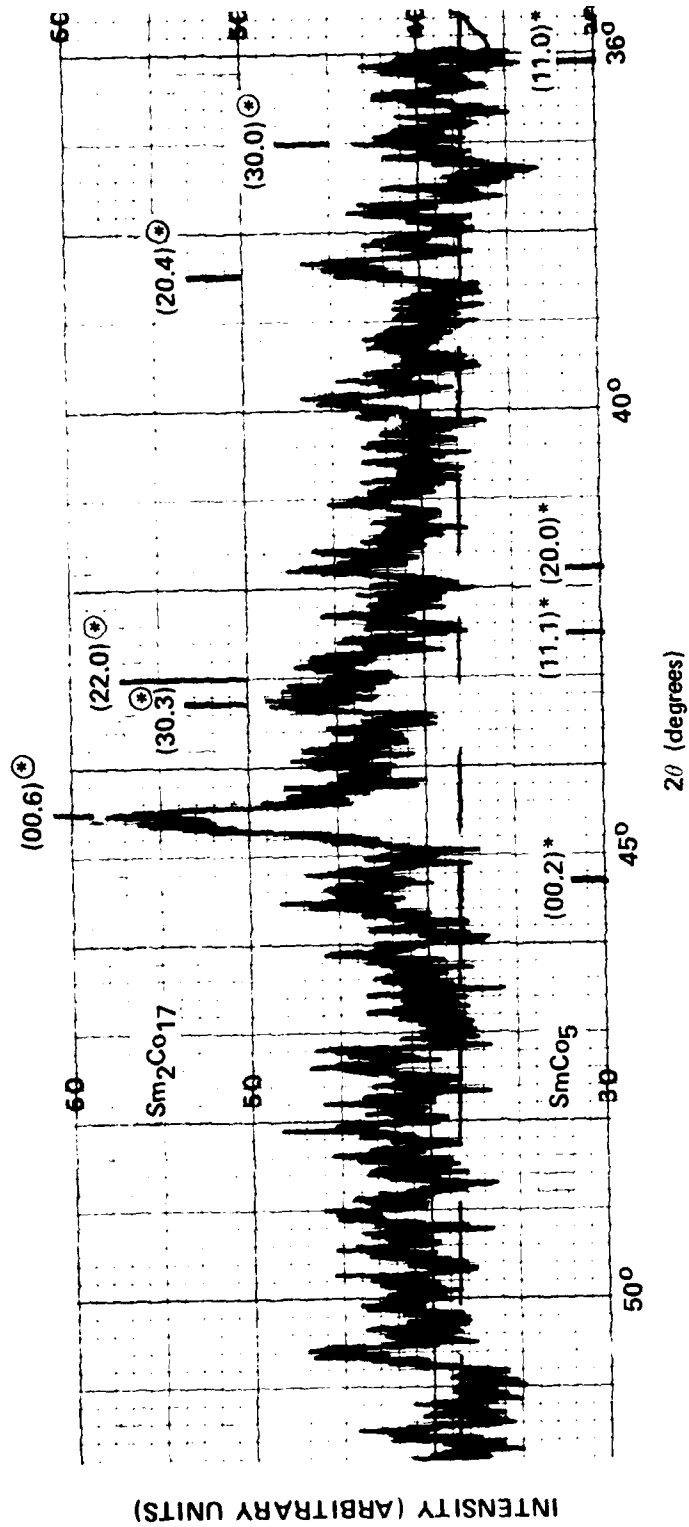
X-ray diffraction patterns were obtained on a few of the deposits fabricated with 34.0 and 30.0 weight percent Sm powder. The diffraction patterns were obtained on the flat side of the deposit closest to the substrate since that had experienced the most severe cooling during deposition. Plasma spraying is known to result in amorphous and metastable crystalline structures^(22,23) and the intention was to see if an amorphous material was obtained with these compositions. The diffraction patterns obtained on three such samples are shown in Figure 11. Also included in Figure 11 are peak positions for well-crystallized SmCo_5 and $\text{Sm}_2\text{Co}_{17}$ intermetallic compounds. All of the x-ray patterns were obtained with copper radiation and a diffracted beam graphite monochromator.

Considerable broadening of the x-ray peaks was observed for all of the deposits. The diffuse patterns obtained on these materials are believed to be indicative of amorphous structures similar to what are conventionally obtained by rapid quenching techniques. The existence of a few minor crystalline peaks was interpreted to indicate the existence of a small amount of crystalline material dispersed in an otherwise amorphous material. Along these lines a most interesting, and possibly very significant, observation was made for one of the subsequently deposited 34.0 samples. The x-ray pattern obtained from the surface of this sample (shown in Figure 12) consisted of a single, sharp crystalline peak superposed on an otherwise amorphous type pattern. A single peak was interpreted as illustrative of texture in the crystalline component of the deposit. This deposit was fabricated using a starting composition of 34.0 weight percent Sm. The composition of the deposit was indicated to be about 30.0 weight percent Sm (which is in the two-phase SmCo_5 - $\text{Sm}_2\text{Co}_{17}$ region of the phase diagram), by x-ray fluorescence. The sole crystalline peak observed was found to be located at the (00.6) peak position for $\text{Sm}_2\text{Co}_{17}$ - the compound of interest. This observation showed that it might be possible to produce crystallographically aligned $\text{Sm}_2\text{Co}_{17}$ materials by plasma spraying, a feature that has so far eluded efforts on the SmCo_5 sprayed materials.



2/81 CD22661 REV A

Figure 11. As-sprayed x-ray patterns obtained on two deposits made with 34 wt % Sm and one with 30 wt % Sm powders. Expected peak positions are identified for SmCo₅ and Sm₂Co₁₇ compounds using the symbols * and ⊙ respectively.



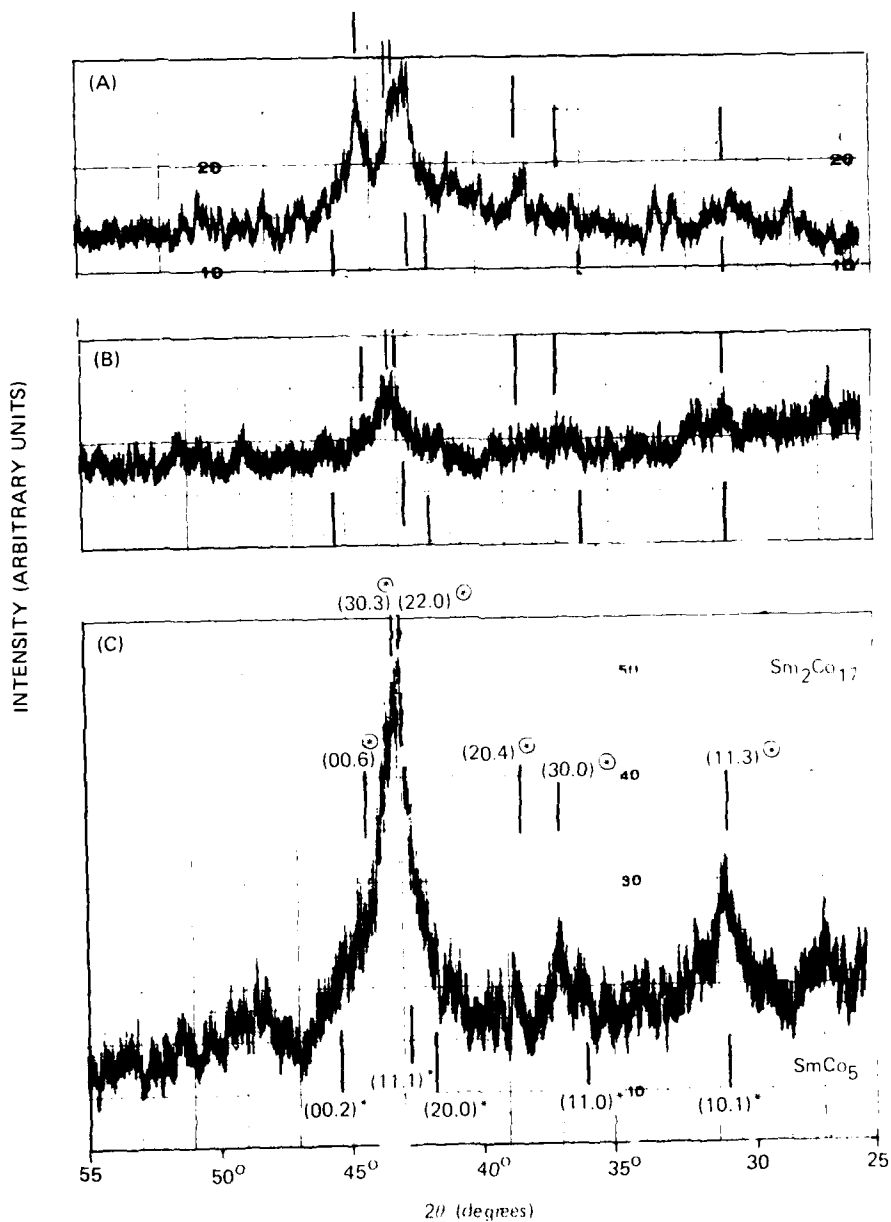
2/81 CD22589 REV A

Figure 12. X-ray pattern showing single, sharp crystalline peak superposed on an essentially amorphous pattern. Expected peak positions for SmCo₅ and Sm₂Co₁₇ compounds are indicated by the symbols * and ⊙ respectively.

Subsequent efforts at producing similar material for detailed examination have met with limited success. It appears that small changes in the cooling rate of the deposited material (induced by minor variations in experimental conditions) will affect the structure of the deposit. (Attempts are presently underway to vary the cooling conditions at the substrate.) In one instance, however, a somewhat more crystalline (possibly microcrystalline) deposit was obtained with a strong (00.6) peak. When a portion of this deposit was removed, crushed into the form of a powder and subjected to x-ray diffraction, an amorphous type pattern was observed with none of the peaks clearly identified. The (00.6) peak was found to almost disappear, indicating that the strong peak observed earlier corresponded to Bragg reflections from a relatively small volume of crystalline material that existed in the form of oriented crystallites, thereby reinforcing the total (00.6) reflection. The process of reducing the deposit into a fine powder must have resulted in producing overall random orientation of these crystallites and this showed up as a significantly reduced intensity. Both of these patterns are shown in Figure 13. This figure also contains the pattern obtained on another section of the solid as-deposited material which was subjected to a temperature of 550°C for 16 hours in argon. An increased degree of crystallinity resulted from this treatment. This was expected from past experience. (23)

4.5.5 Heat Treatment and Magnetic Properties

A few discs, each 0.200 inch in diameter, were cored from each of the deposited materials using electrical discharge machining (EDM). The magnetic properties were measured for the as-sprayed condition on one set of discs. The several discs were then subjected to a series of different heat treatment conditions and the properties measured using maximum applied static magnetic fields up to 140 kOe. Both temperature as well as time at temperature were varied and the effects resulting from such treatments are discussed below.



2/81 CD22660 REV A

Figure 13. X-ray patterns of film deposited sample: (A) As-deposited; (B) After grinding to fine powder; (C) 550°C, 10 hrs. anneal.

4.5.5.1 Effect of Temperature

A series of exposures at successively higher temperatures were employed for the several deposited samples. Time at each temperature was fixed at 16 hours. After each thermal exposure the power to the furnace was shut off and the heat-treated discs allowed to cool slowly inside the furnace. The magnetic properties measured after the different heat treatments are listed in Table 9. This table also shows the properties measured on these materials after a high temperature exposure of 1100°C followed by an aging treatment at 850°C. (Temperatures far in excess of 1100°C are used when sintering is employed as the fabrication process). The observed variation of H_{c1} with temperature of exposure is further plotted in Figure 14.

4.5.5.2 Effect of Time at Temperature

Another set of as-sprayed discs was next exposed to varying time at a fixed temperature of 600°C. Again, as before, the power to the furnace was shut off after each exposure and the heat-treated samples allowed to cool slowly inside the furnace. The magnetic properties measured after these latter treatments are shown in in Table 10. The variation of H_{c1} with time of exposure is shown in Figure 15.

Several interesting observations were made from the tabulated and plotted magnetic data. These are briefly discussed below.

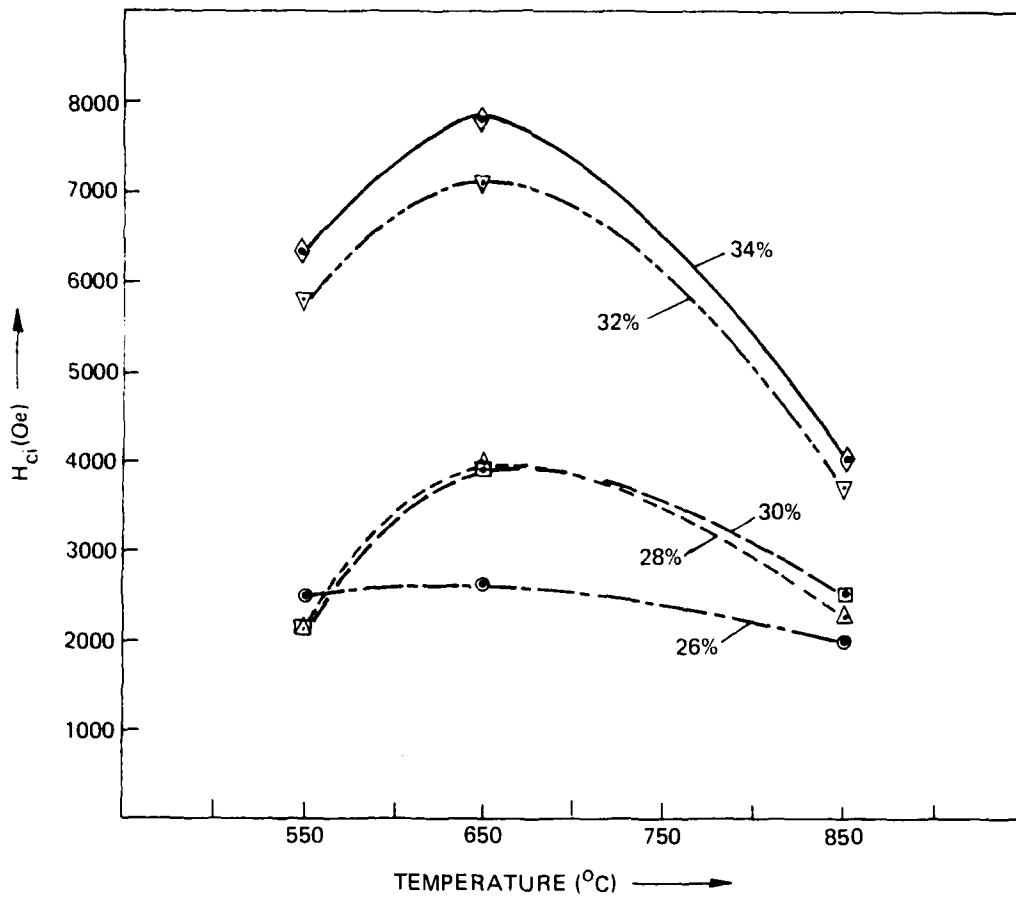
- (1) Substantial improvements were observed for the magnetic properties with the low temperature treatments. These were attributed to increased homogenization and grain growth through crystallization-related processes.

Table 9. Effect of temperature of treatment.

Sample	Heat Treatment	B_r (G)	$4\pi M_D$ (G)*	H_C (Oe)	H_{Ci} (Oe)	(BH) _{max} (MGOe)
34.0	(A) : As-sprayed	5800	9100	1700	2400	2.5
32.0		5600	8750	2300	4250	3.2
30.0		4700	8350	2300	3800	2.7
28.0		6650	10000	1500	2100	2.5
26.0		4300	10300	1000	1300	1.6
34.0	(A) + (B) : 550°C, 16 hrs	5750	8600	3150	6300	4.5
32.0		5750	8500	2850	5850	4.1
30.0		5600	9800	1400	2050	3.5
28.0		5950	9550	1500	2100	2.2
26.0		5100	8500	1850	2500	2.4
34.0	(A) + (B) + (C) : 650°C, 16 hrs	5900	7400	4100	7800	6.0
32.0		6000	7450	3900	7150	6.0
30.0		5950	8700	2600	3900	4.0
28.0		6100	8700	2700	4000	4.0
26.0		5250	8450	2000	2600	3.0
34.0	(A) + (B) + (C) (D) : 850°C, 16 hrs	5300	6900	2750	4000	3.5
32.0		5300	6950	2650	3700	3.5
30.0		5550	7900	1800	2500	2.5
28.0		5550	7950	1900	2300	2.5
26.0		5050	8200	1600	2000	2.0
34.0	(A) + (B) + (C) + (D) : 1100°C, 2 hrs; 850°C, 24 hrs	3500	6600	1200	1800	1.0
32.0		3700	6600	1200	1900	1.1
30.0		3450	7650	600	700	0.5
28.0		3200	7460	600	600	0.5
26.0		2050	7500	400	500	0.2

* $4\pi M$ value at 15 kOe field strength on demagnetization portion of $4\pi M$ versus H curve.

2/81 CD22601



2/81 CD22566

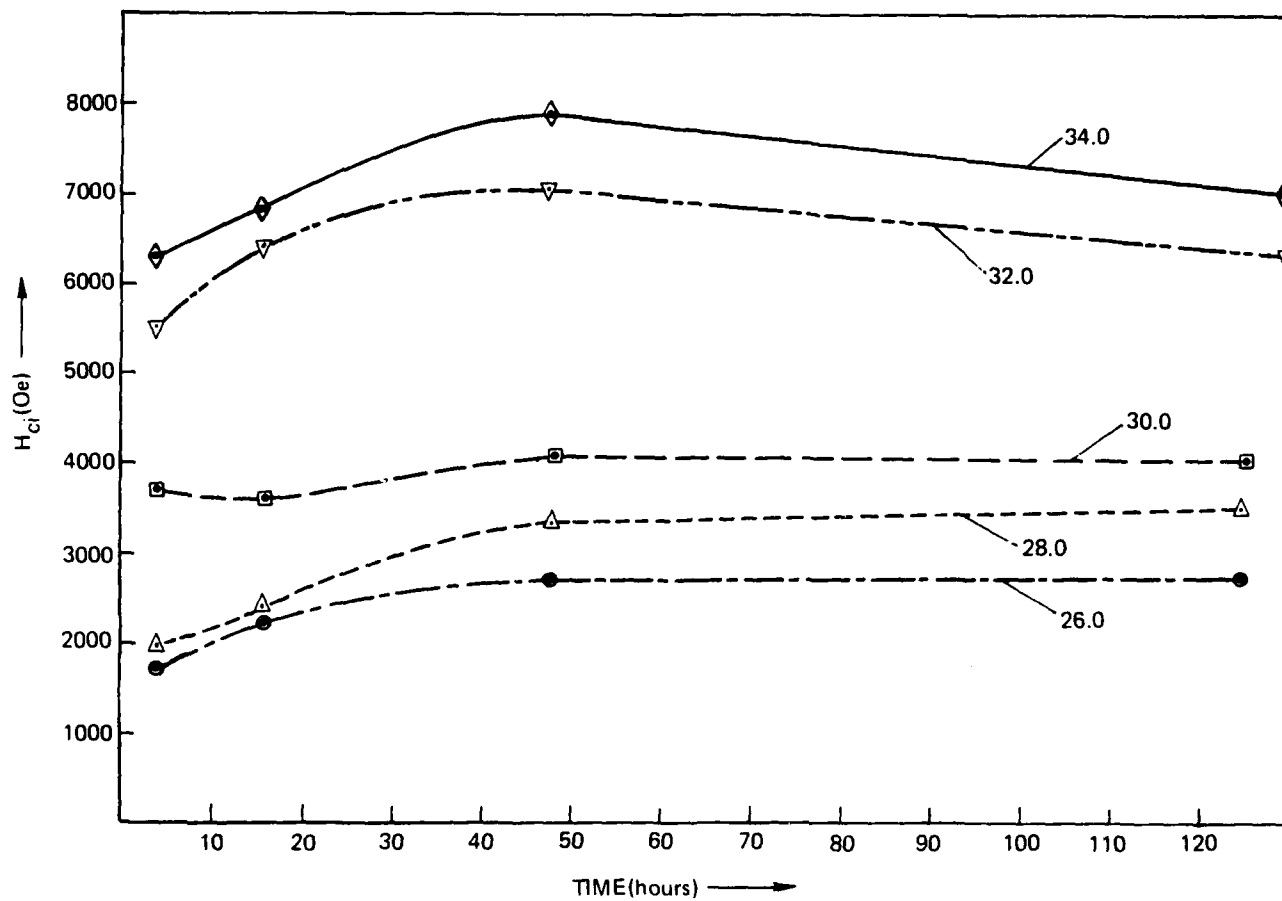
Figure 14. Effect of temperature of treatment on H_{ci} (for fixed time = 16 hours).

Table 10. Effect of time at temperature.

Sample	Heat Treatment	B_r (G)	$4\pi M_D$ (G) *	H_C (Oe)	H_{ci} (Oe)	(BH) _{max} (MGoe)
34.0	(A): As-sprayed +	6400	8650	2900	6300	4.7
32.0	(B): 600°C, 4 hrs	6300	8600	2700	5500	4.3
30.0		5600	8300	2400	3700	3.4
28.0		6350	9700	1500	2000	2.4
26.0		5550	10230	1200	1700	1.7
34.0	(A) + (B) +	5900	7950	3100	6800	4.0
32.0	(C): 600°C, 12 hrs	6300	8350	3100	6400	4.9
30.0		5300	8100	2300	3600	3.0
28.0		5600	9050	1700	2400	2.4
26.0		5500	9700	1600	2200	2.2
34.0	(A) + (B) + (C) +	6500	8200	4050	7900	6.6
32.0	(D): 600°C, 32 hrs	6500	8350	3700	7050	6.0
30.0		5900	8500	2700	4100	4.0
28.0		6550	9400	2300	3400	3.8
26.0		5900	9750	1900	2700	2.8
34.0	(A) + (B) + (C) +	6450	8000	4100	7000	6.6
32.0	(D) + (E): 600°C,	6650	8100	3850	6300	6.4
30.0	77 hrs	5800	8250	2650	4000	3.8
28.0		6150	8900	2550	3500	3.9
26.0		5700	9350	2050	2700	2.9

* $4\pi M$ value at 15 kOe field strength on the demagnetization portion of the $4\pi M$ versus H curve.

2/81 CD22599



2/81 CD22565

Figure 15. Effect of time of exposure at 600°C on the value of H_{Ci} .

- (2) Unlike observations on similarly produced modified $\text{Sm}_2\text{Co}_{17}$ -type compositions,⁽²⁴⁾ the dependence of the thermal treatment required (for producing optimum coercivity) on deposit composition was found to be at best minimal. These observations indicated that grain size played a strong role in determining H_{ci} of these binary compositions.
- (3) The largest value of H_{ci} measured for these binary Sm-Co compositions in this program was 7.9 kOe.
- (4) The high values measured for $4\pi M_D$ in the as-sprayed condition were indicative of the amorphous nature of these deposits. As expected, these values were found to gradually decrease with increasing crystallization, which resulted from the heat treatments that were performed.

4.6 Conclusions

H_{ci} values of up to 8 kOe were generated in binary $\text{Sm}_2\text{Co}_{17}$ -type compositions by using appropriately selected, low temperature heat treatments on amorphous and close-to-amorphous plasma-sprayed deposits. It was determined that amorphous material (over a reasonably broad range of composition) could be produced using this technique in agreement with earlier observations.⁽²²⁾ The possibility of producing $\text{Sm}_2\text{Co}_{17}$ -type magnets with the easy magnetization axis oriented perpendicular to the plane of the deposit was indicated in this study. The existence of a sole crystalline peak, superimposed on an amorphous pattern and located at the expected peak position for the (00.6) reflection from $\text{Sm}_2\text{Co}_{17}$, was interpreted as indicating texture in the deposit. These suspicions were confirmed in that this peak was observed to all but disappear when a powder pattern of this material was obtained. It was concluded that the cooling conditions at the substrate significantly affected the texture in the deposit.

4.7 Recommendations for Future Work

- (1) Vary cooling conditions at the substrate to study influence on deposit structure.
- (2) Examine effects of crystallizing the amorphous materials in the presence of externally applied magnetic fields and thermal gradients.
- (3) Study the influence of low temperature crystallization treatments in an hydrogen atmosphere.

REFERENCES

1. Das, D., E. Wettstein, and K. Kumar, Technical Report R-1177, Charles Stark Draper Laboratory, July 1978. Office of Naval Research Contract N00014-77-C-0388.
2. Das, D., K. Kumar, and E. Wettstein, Technical Report R-1306, Charles Stark Draper Laboratory, October 1979. Office of Naval Research Contract N00014-77-C-0388.
3. Benz, M.G., R.P. Laforce, and D.L. Martin, AIP Conf. Proc. No. 18, p. 1173, 1974.
4. Mildrum, H.F., and D.J. Iden, Goldschmidt Informiert, 4/75, No. 35, p. 54, December 1975.
5. Livingston, J.D., AIP Conf. Proc. No. 10, p. 643, 1973.
6. Bartlett, R.W., and P.J. Jorgensen, J. Less Common Metals, 37, p. 21, 1974.
7. Kumar, K., D. Das, and E. Wettstein, J. Appl. Phys., 49 (3), p. 2052, 1978.
8. Das, D., and K. Kumar, Proc. 3rd Int'l Workshop on RE-Co Magnets, p. 494, University of California, San Diego, 1978.
9. Benz, M.G., and D.L. Martin, J. Appl. Phys., 43 (7), p. 3165, 1972.
10. Mildrum, H.F., and K.D. Wong, Proc. 2nd Int'l Workshop on RE-Co Magnets, p. 35, Dayton, Ohio, 1978.
11. Tatsumoto, E., et al, Jnl. de Physique, v. 32, p. CI-550, 1971 Supple.

12. Okamoto, T., et al, J. Phys. Soc., Japan, 34, p. 835, 1973.
13. Jones, F.G., and M. Tokunaga, IEEE Trans., Magnetics, Vol. Mag-12, No. 6, p. 968, November 1976.
14. Kumar, K., Tech Rept. C-4617, Charles Stark Draper Laboratory, Cambridge, Massachusetts, April 1976.
15. Das, D., IEEE Trans. Magn., MAG 5 (3), p. 214, 1969.
16. Bachmann, K., and H. Nagel, Proc. 2nd Int'l Workshop on RE-Co Magnets, Dayton, Ohio, 1976.
17. Strnat, K.J., and A.E. Ray, Goldschmidt informiert, 4/75, p. 47, 1975.
18. Benz, M.G., and D.L. Martin, in Technical Report AFML-TR-72-29, Wright-Patterson Air Force Base, Ohio, 1972. (Research performed at GE R&D Center, Schenectady.)
19. Kumar, K., D. Das, and E. Wettstein, IEEE Trans. Magn., MAG-14 (5), p. 788, 1978.
20. Kumar, K., and D. Das, J. Appl. Phys., 50 (4), p. 2940, 1979.
21. Kumar, K., D. Das, and C.R. Dauwalter (unpublished).
22. Kumar, K., and D. Das, Thin Solid Films, 54 (3), p. 263, 1978.
23. Kumar, K., D. Das, and R. Williams, J. Appl. Phys., 51 (2), p. 1031, 1980.
24. Kumar, K., Technical Report R-1419, Charles Stark Draper Laboratory, October 1980.

BASIC DISTRIBUTION LIST

<u>Organization</u>	<u>Copies</u>	<u>Organization</u>	<u>Copies</u>
Defense Documentation Center Cameron Station Alexandria, VA 22314	12	Naval Air Propulsion Test Center Trenton, NJ 08628 ATTN: Library	1
Office of Naval Research Department of the Navy 800 N. Quincy Street Arlington, VA 22217		Naval Construction Batallion Civil Engineering Laboratory Port Hueneme, CA 93043 ATTN: Materials Division	1
ATTN: Code 471	1	Naval Electronics Laboratory San Diego, CA 92152 ATTN: Electron Materials Science Division	1
Code 102	1		
Code 470	1		
Commanding Officer Office of Naval Research Branch Office Building 114, Section D 666 Summer Street Boston, MA 02210	1	Naval Missile Center Materials Consultant Code 3312-1 Point Mugu, CA 92041	1
Commanding Officer Office of Naval Research Branch Office 536 South Clark Street Chicago, IL 60605	1	Commanding Officer Naval Surface Weapons Center White Oak Laboratory Silver Spring, MD 20910 ATTN: Library	1
Office of Naval Research San Francisco Area Office 760 Market Street, Room 447 San Francisco, CA 94102	1	David W. Taylor Naval Ship Research and Development center Materials Department Annapolis, MD 21402	1
Naval Research Laboratory Washington, DC 20375		Naval Undersea Center San Diego, CA 92132 ATTN: Library	1
Attrn: Codes 6000	1	Naval Underwater System Center Newport, RI 02840 ATTN: Library	1
6100	1		
6300	1		
6400	1		
2627	1	Naval Weapons Center China Lake, CA 93555 ATTN: Library	1
Naval Air Development Center Code 302 Warminster, PA 18964 ATTN: Mr. F.S. Williams	1	Naval Postgraduate School Monterey, CA 93840 ATTN: Mechanical Engineering Department	1

BASIC DISTRIBUTION LIST (Continued)

<u>Organization</u>	<u>Copies</u>	<u>Organization</u>	<u>Copies</u>
Naval Air Systems Command Washington, DC 20360 ATTN: Codes 52031 52032	1	NASA Headquarters Washington, DC 20546 ATTN: Code KRM	1
Naval Sea System Command Washington, DC 20362 ATTN: Code 035	1	NASA (216) 433-4000 Lewis Research Center 21000 Brookpark Road Cleveland, OH 44135 ATTN: Library	1
Naval Facilities Engineering Command Alexandria, VA 22331 ATTN: Code 03	1	National Bureau of Standards Washington, DC 20234 ATTN: Metallurgy Division Inorganic Materials Division	1 1
Scientific Advisor Commandant of the Marine Corps Washington, DC 20380 ATTN: Code AX	1	Director Applied Physics Laboratory University of Washington 1013 Northeast Fortieth Street Seattle, WA 98105	1
Naval Ship Engineering Center Department of the Navy Washington, DC 20360 ATTN: Code 6101	1	Defense Metals and Ceramics Information Center Battelle Memorial Institute 505 King Avenue Columbus, OH 43201	1
Army Research Office P.O. Box 12211 Triangle Part, NC 27709 ATTN: Metallurgy and Ceramics Program	1	Metals and Ceramics Division Oak Ridge National Laboratory P.O. Box X Oak Ridge, TN 37380	1
Army Materials and Mechanics Research Center Watertown, MA 02172 ATTN: Research Programs Office	1	Los Alamos Scientific Laboratory P.O. Box 1663 Los Alamos, NM 87544 ATTN: Report Librarian	1
Air Force Office of Scientific Research Bldg. 410 Bolling Air Force Base Washington, DC 20332 ATTN: Chemical Science Directorate	1	Argonne National Laboratory Metallurgy Division P.O. Box 229 Lemont, IL 60439	1
Electronics & Solid State Sciences Directorate	1	Brookhaven National Laboratory Technical Information Division Upton, Long Island New York 11973 ATTN: Research Library	1
Air Force Materials Laboratory Wright-Patterson AFB Dayton, OH 45433	1		

BASIC DISTRIBUTION LIST (Continued)

<u>Organization</u>	<u>Copies</u>	<u>Organization</u>	<u>Copies</u>
Library Building 50, Room 134 Lawrence Radiation Laboratory Berkeley, CA	1	Office of Naval Research Branch Office 1030 East Green Street Pasadena, CA 91106	1

SUPPLEMENTARY DISTRIBUTION LIST

Technical and Summary Reports

Professor Albert E. Miller
University of Notre Dame
Box 8
Notre Dame, IN 46556

Professor Karl J. Strnat
University of Dayton
Magnetic Laboratory
Dayton, OH 45469

Dr. J.J. Becker
General Electric Research
and Development Center
P.O. Box 8
Schenectady, NY 12301

Professor W.E. Wallace
Department of Chemistry
University of Pittsburgh
Pittsburgh, PA 15213

Dr. Richard P. Allen
Battelle-Northwest
Richland, WA 99352

Dr. Howard T. Savage
Naval Surface Weapons Center
White Oak
Silver Spring, MD 20910

Mr. Harold Garrett
Air Force Materials Laboratory
LTE, Bldg. 16
Wright-Patterson Air Force Base
Dayton, OH 45433

Dr. L.D. Jennings
Army Materials and Mechanics
Research Center
Watertown, MA 02172

Dr. J.O. Dimmock, Director
Electronic and Solid State
Sciences Program (Code 427)
Office of Naval Research
Arlington, VA 22217

Assistant Chief for Technology
(Code 2000)
Office of Naval Research
Arlington, VA 22217

Strategic Systems Projects Office
Department of the Navy
Washington, DC

Professor G.S. Ansell
Rensselaer Polytechnic Institute
Dept. of Metallurgical Engineering
Troy, NY 12181

Dr. David L. Martin
General Electric Research
and Development Center
P.O. Box 8
Schenectady, NY 12301

Professor M. Cohen
Massachusetts Institute of Technology
Department of Metallurgy
Cambridge, MA 02139

Professor J.W. Morris, Jr.
University of California
College of Engineering
Berkeley, CA 94720

Professor O.D. Sherby
Stanford University
Materials Sciences Division
Stanford, CA 94300

SUPPLEMENTARY DISTRIBUTION LIST (Continued)

Dr. E.A. Starke, Jr.
Georgia Institute of Technology
School of Chemical Engineering
Atlanta, GA 30332

Professor David Turnbull
Harvard University
Division of Engineering and
Applied Physics
Cambridge, MA 02139

Dr. D.P.H. Hasselman
Montana Energy and MHD Research
and Development Institute
P.O. Box 3809
Butte, MT 59701

Dr. L. Hench
University of Florida
Ceramics Division
Gainesville, FL 32601

Dr. J. Ritter
University of Massachusetts
Department of Mechanical
Engineering
Amherst, MA 01002

Professor J.B. Cohen
Northwestern University
Dept. of Material Sciences
Evanston, IL 60201

Director
Materials Sciences
Defense Advanced Research
Projects Agency
1400 Wilson Boulevard
Arlington, VA 22209

Professor H. Conrad
University of Kentucky
Materials Department
Lexington, KY 40506

Dr. A.G. Evans
Dept. of Material Sciences
and Engineering
University of California
Berkeley, CA 94720

Professor H. Herman
State University of New York
Material Sciences Division
Stony Brook, NY 11794

Professor J.P. Hirth
Ohio State University
Metallurgical Engineering
Columbus, OH 43210

Professor R.M. Latanision
Massachusetts Institute of Technology
77 Massachusetts Avenue
Room E19-702
Cambridge, MA 02139

Dr. Jeff Perkins
Naval Postgraduate School
Monterey, CA 93940

Dr. R.P. Wei
Lehigh University
Institute for Fracture and
Solid Mechanics
Bethlehem, PA 18015

Professor G. Sines
University of California
at Los Angeles
Los Angeles, CA 90024

Professor H.G.F. Wilsdorf
University of Virginia
Department of Materials Science
Charlottesville, VA 22903

Dr. A. Tauber
Dept. of the Army
HQ, U.S. Army Electronic Command
Fort Monmouth, NY 07703

SUPPLEMENTARY DISTRIBUTION LIST (Continued)

Mr. K.K. Jin
Strategic Systems Division
Autonetics Group
3370 Miraloma Avenue
P.O. Box 4192
Anaheim, CA 92803

National Magnet Laboratory
Massachusetts Institute of Technology
145 Albany Street
Cambridge, MA 02139
ATTN: Dr. Donald T. Stevenson (2)
Assistant Director

Mr. N. Horowitz
The Aerospace Corporation
2350 East El Segundo Boulevard
El Segundo, CA

Dr. C.W. Chang
G.E. Valley Forge Space Center
P.O. Box 8555
Philadelphia, PA 19101

Mr. Francis W. Wessbecher
Unit Head
Inertial Component Engineering
Singer Kearfott Division
150 Totowa Road
Wayne, NJ 07470

Mr. Carl Flom
Delco Electronics
7929 South Howell
Box 471
Milwaukee, WI 53201

K. Narasimhan/C.D. Preusch
Crucible Research Center
P.O. Box 88
Pittsburgh, PA 15230

DATE
ILMED
-8